

ACTA UNIVERSITATIS SZEGEDIENSIS

PARS CLIMATOLOGICA
SCIENTIARIUM NATURALIUM
CURAT: JÁNOS UNGER

ACTA CLIMATOLOGICA

TOMUS LIV.

SZEGED (HUNGARIA)

2020

Editor-in-chief

JÁNOS UNGER

Editorial board

ILONA BÁRÁNY-KEVEI

ANITA BOKWA

TAMÁS GÁL

ÁGNES GULYÁS

MÁRTON KISS

PAVEL KONSTANTINOV

ATTILA KOVÁCS

RÓBERT MÉSZÁROS

STEVAN SAVIĆ

NÓRA SKARBIT

Technical editor

TAMÁS GÁL

Publisher

University of Szeged, Faculty of Science and Informatics
(H-6720 Szeged, Aradi vértanúk tere 1.)

The issues are available on
www.clima.u-szeged.hu/acta-climatologica

Acta Universitatis Szegediensis: **ISSN 0324-6523**

Acta Climatologica: **ISSN 0563-0614**

CONTENTS

Csete ÁK, Gulyás Á: Adaptation of UFORE-Hydro model for Szeged and the southern region of the Great Hungarian Plain based on local meteorological database	5
Unger J, Skarbit N, Gál T: Projection of present and future daily and evening urban heat load patterns	19
Guo Y, Gál T, Tian G, Li H, Unger J: Model development for the estimation of urban air temperature based on surface temperature and NDVI – a case study in Szeged.....	29
Unger J: Urban heat island studies in Szeged, Hungary – An overview based on papers published over the past forty years (1980–2020)	41

ADAPTATION OF UFORE-HYDRO MODEL FOR SZEGED AND THE SOUTHERN REGION OF THE GREAT HUNGARIAN PLAIN BASED ON LOCAL METEOROLOGICAL DATABASE

Á K CSETE and Á GULYÁS

*Department of Climatology and Landscape Ecology, University of Szeged, Egyetem u. 2., 6720 Szeged, Hungary
E-mail: cseteakos@geo.u-szeged.hu*

Summary: Urban environments are very different from natural ones in many cases. The geometry of the buildings and the various artificial surface elements can significantly influence the microclimatic and hydrological processes. In urban areas, the surface is mostly artificial and it is hard to find natural, undisturbed surfaces, in addition, the vast majority of soil surfaces are generally under strong anthropogenic influence. Models can provide a comprehensive view of the hydrological processes in the city and can help to investigate the different impacts of them. In this study, our aim is to introduce the preparation of a widely applicable model (UFORE-Hydro) for Hungarian pilot areas. Thus, we intend to introduce the procedure of preparing the weather and evaporation files and their local databases which we used for the model.

Key words: urban hydrology, i-Tree Hydro, sustainable urban water management, green infrastructure, nature-based solutions

1. INTRODUCTION

Growing urban areas and the increasing number of urban citizens are the results of urbanization which is one of the greatest challenges of the 21st century. Nowadays, the worldwide proportion of urban population is over 54%, which is gradually increasing and could reach 66% by 2050 (UN DESA 2019). The territorial and population growth is accompanied by changes in the natural environment and the spread of townscape. The problems of urban areas cannot be separated from the future effects of climate change. Among the negative effects of climate change, urban water volume and its time distribution is a major problem, which is even more relevant in connection with the growing urban population.

Urban environment shows a fundamentally different picture compared to natural areas. The geometry of the buildings as well as the various artificial surface cover elements can significantly influence the microclimatic and hydrological processes. The most significant change in land cover is the increase of built-up areas, including the use of artificial, mostly impervious pavements (e.g. concrete, asphalt, bricks, various stone pavers, etc.). Furthermore, the major part of soils is usually under strong anthropogenic effects (e.g. soil sealing, compacting). These factors can significantly affect the hydrological sub-processes. The most important side effect of impervious surfaces is that they significantly increase surface drainage ability, thus surface runoff (Department of Water 2007, Gayer and Ligetvári 2007).

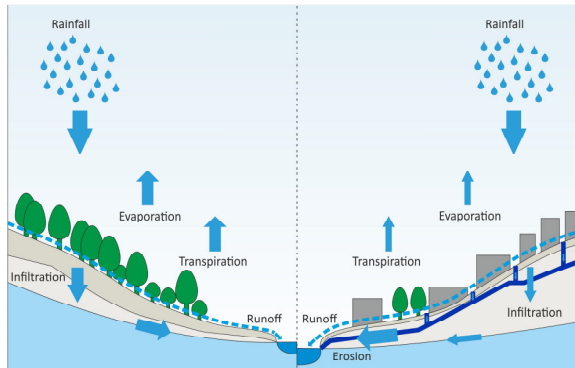


Fig. 1 The route of water in urban and natural areas (based on [2])

In urban watersheds, the route of precipitation that actually reaches the surface differs significantly from natural areas. The afore-mentioned impervious surfaces do not allow water to infiltrate into the deeper layers. The primary reason for this is the presence of impervious pavements; the other is the drainage system, of which primary purpose is to drain the excess water as quickly as possible. Compared to natural areas, temporary or long-term storage does not occur in urban areas. Due to the rapid drain ability of the impervious surfaces, watercourses flowing through urban areas are exposed to the significant impact of erosion (Fig. 1). Nevertheless, the real problem is the increase in surface runoff volumes. In case large amount of precipitation furthermore, if there is an undersized sewer network, there is a high chance of an urban flashflood (Fig. 2). In a short-term, heavy rainfall event, surface runoff may also reach 80-90% for pervious surfaces, which may be even higher in the case of paved surfaces (Buzás 2012).

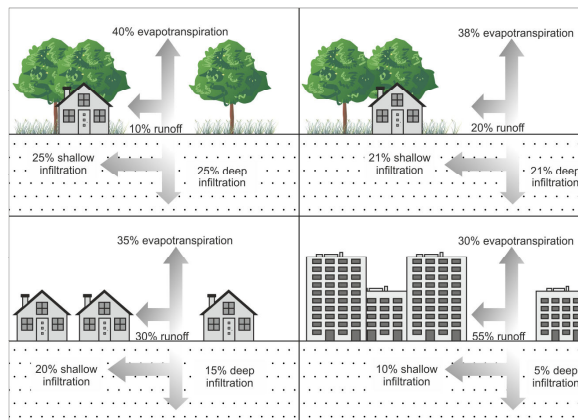


Fig. 2 Hydrological processes of different built-up areas (based on US EPA 2003)

In the sustainable urban water management, green infrastructure – as a nature-based solutions (NBS) – plays a key role, within which woody vegetation (trees) has a particular importance for urban ecology (Romnée at al. 2015, Raymond et al. 2017). Trees, among others, participate in the more efficient utilization of precipitation (e.g. runoff reduction, increase in infiltration), influence the microclimate of a city in a positive direction, and play

a significant role in pollution sequestration (Xiao and McPherson 2002, Berland et al. 2017). Due to their size and physiological properties, their importance in water management is significant compared to other vegetation types, because they are able to interact with precipitation on a larger surface. As a result, they significantly reduce surface runoff, which is a key issue for urban areas with predominantly impervious surfaces. The large amount of rainwater, which is stored in the trunk, branches, and in the tree canopy, also significantly influences the micro-climatic characteristics (e.g. humidity) (Fletcher et al. 2015, Berland et al. 2017).

For these reasons, examining the role of urban vegetation in water management is a very actual issue. Considering growing urban population and the increasing frequency of intense rainfall events, there is an increasing need to change the traditional urban water management approach (which did not focus on vegetation in the past), as global trends are increasingly showing the potential how urban vegetation can and should be used in water management. It is evidenced by the increasingly widespread use of modern water management systems (e.g. WSUD in Australia) and design projects focusing on water retention (e.g. the “Sponge City” project in Berlin, China, and Taiwan) (Liu et al. 2015). Researches in this scientific area are still relatively rare in Hungary, so we find it particularly important to support the claims with more accurate data and model calculations, which are valid for Hungarian conditions and can help to consider green infrastructure as an opportunity for local decision-making processes (Buzás 2012). Therefore, the central element of our study helps the adaptation of a widely applicable model (UFORE-Hydro) to Hungarian study sites. The model is available as part of the i-Tree model family developed in the US, and it is outstanding in many respects, as it focuses on the impact of vegetation on urban hydrology (Kimbauer et al. 2013, Jayasooriya and Ng 2014, Nowak et al. 2018).

The purpose of this work is to present the methodological steps that help the adaptation of the model to the Hungarian circumstances. Furthermore, we intend to present the procedure of the complex input data preparation (weather and evaporation data files) used in the model, based on the Hungarian databases. We would also like to draw the attention of Hungarian decision-makers to the diverse opportunities in the application of urban green infrastructure combined with urban water management. Our data processing steps and results can support the work of professional and scientific experts who can contribute to the decision-making processes.

2. APPLICATION OF THE UFORE-HYDRO MODEL

The UFORE-Hydro model accessible as a part of i-Tree model family (the model can be run through the computer interface of the i-Tree Hydro program, hence referred to as Hydro). The model was developed in the US by various institutes (SUNY College of Environmental Science and Forestry, USDA Forest Service, Syracuse University and the Davey Institute) (Yang et al. 2011, Kimbauer et al. 2013, Jayasooriya and Ng 2014, Nowak et al. 2018). The Hydro is an ideal tool for analysis different areas and land cover scenarios as well as their hydrological impacts. It can be use at various scales, from a part of urban watershed to a whole city. The advantage of the UFORE-Hydro model (in comparison with other stormwater models), that it can simulate the effect of changes in urban vegetation and its impact on the urban hydrological system more detailed. Most of the urban hydrological

model cannot handle the different types of vegetation and other features (LAI, leaf-off day, etc.).

Among the outputs of the model, information can be obtained about the total runoff, including the base flow, and the two components of the surface runoff: the flow of impervious surfaces and the flow of pervious surfaces. The effect of vegetation on the runoff can be concluded from the data of interception, evaporation, canopy storage, and infiltration.

The model consists of two main input data sources: meteorological and spatial data. When providing meteorological data, we need to create a weather file and an evaporation file, which will be detailed in the next chapter.

When specifying spatial data, we need a terrain model that allows the model to calculate the direction of the surface flow and its accumulation locations. However, the most important spatial data relate to the land cover of the sites. The percentage of land cover data should include the following: tree canopy cover, herbaceous vegetation cover, shrub vegetation cover, open soil surfaces, water surfaces, and impervious surfaces (buildings and pavements). Additional data are also required for tree canopy and shrub vegetation, as the surface cover beneath their canopy of these types may vary by area. Therefore, it is necessary to define the proportion of impervious and pervious surfaces beneath them. Within both types, we also need to define the spatial distribution of evergreen species.

To define the land cover categories, we used eCognition 9.1 Developer (Baatz and Schape 2000, Manakos et al. 2000, Hay et al. 2005). For this, we used a leafage orthophoto from 2015 and a leafless orthophoto from 2016, in both cases with a geometric resolution of 0.4 meters. We used a digital surface model and a normalized digital surface model (2015) to define the height classes within the vegetation and impervious surfaces. To define these categories, eCognition was used, which requires proper consideration of the spectral and formal characteristics of the data. With Hydro, in addition to real land cover ratio, we have the opportunity to work with alternative land cover ratio, which can be an important tool for urban planning. The real land cover data based on the values of the orthophotos, in contrast with the alternative land cover, where we can define hypothetical land cover rate. In this case, we can run model scenarios and these can be used to estimate the effect of a future square renovation or greening.

For the international use of the Hydro model, in the previous studies it is necessary to designate a reference city with similar climatic conditions in the US, where the most important temporal and spatial distribution of climatic parameters are similar to Szeged or other Hungarian cities ([1]). This step was necessary for the model matching. However, with the steps described below, running the model, which is exclusively based on Hungarian databases, now is available, and it will significantly reduce the number of errors. In this work, our aim is to simplify the international use of the model, especially for Hungarian cities.

2.1. Selection of the study areas

Our study sites are in the city of Szeged, which is the center of the southern region of the Great Hungarian Plain with its special climatic conditions. The area is characterized by low annual precipitation (497 mm), high sunshine duration and consequently frequent drought (Balázs et al. 2009). However, while precipitation is relatively low, the intensity of rainfalls varies greatly. Besides, in the summer long drought periods there are frequent flashfloods, which are a major overload for the outdated sewer network and can cause flooding and damage in large areas. Both factors are major challenges for urban water management (Unger and Gál 2017). Four different urban districts were selected in Szeged as

study sites in order to represent the impact of different land cover characteristics on the hydrological character of the areas. When designating the areas, we took into consideration the local climate zones (LCZ) system (complex climatological category system based on surface structure and geometry moreover the thermal and energy features of the surface) applied to Szeged (Unger et al. 2014a, 2014b). In order to achieve better comparability, the area of the study sites are nearly the same.

The description of areas shown below are only needed to present our future examination which based on these methodologies. These areas will be used in other studies, but it is necessary to show them for better understanding the model.

Study site I. is located in LCZ 2, which is characterized by a dense mix of midrise buildings. This area is the most built-up part of Szeged, which can be described as an absolute downtown location. The study site II. is located directly northeast from study site I. Compact installation is also typical in this area, but with low-rise buildings, so this site can be classified as LCZ 3. As a housing estate district, study site III. shows a fundamentally different picture compared to the previous areas. It is located in LCZ 5, which is characterized by open spaces and midrise buildings. Study site IV. is in the southwestern residential part of Szeged. The characteristics of LCZ 6 can be observed here, such as open spaces and low-rise buildings. As it is a relatively newly built part of the city, the arrangement of the buildings follows a very regular, square layout (Fig. 3) (Mucsi et al. 2007, Unger et al. 2014b).

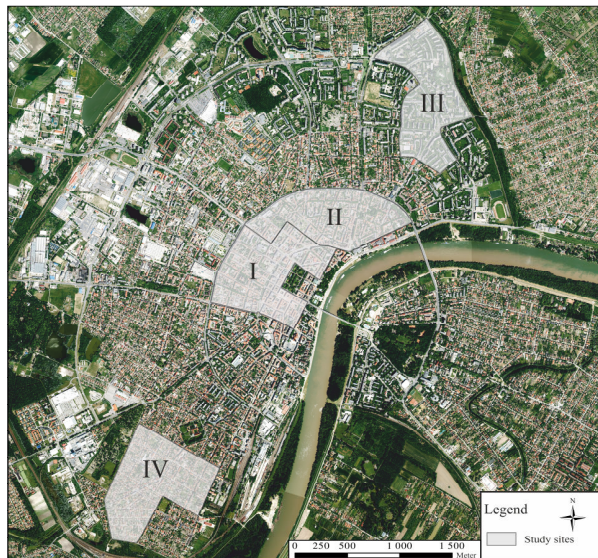


Fig. 3 Study sites within Szeged

2.2. Preparation of the input data

The accurate production of the data in the files is essential to run the model correctly (Wang et al. 2008, [1]). The two files have been produced in the United States so far, which raises accuracy issues (such as the availability of certain national data), on the other hand, it also requires a long waiting time. In order to overcome these problems, we needed to produce the necessary data by ourselves. We used several national databases for the process: the

databases of the Department of Climatology and Landscape Ecology (Szeged) (Unger et al. 2017), the Synoptic Station's database of Hungarian Meteorology Service (HMS Szeged), the SYNOP (Surface Synoptic Observations) database, the i-Tree Eco LAI (Leaf area index) database (run in Szeged) (Kiss et al. 2015), and the ECMWF ERA Interim database (Berrisford et al. 2011).

2.3. Weather file

The weather file forms the basis for the evaporation file, so its accurate production is a top priority (Wang et al. 2008, Hirabayashi and Endreny 2016, [1]). Hydro works with 1-hour resolution data, so the diverse measurement intervals within different databases (10 minutes, 15 minutes) need to be aggregated uniformly. This file contains basic meteorological data that characterize the weather in a given area and time.

The file requires two types of temperature data: air temperature T_{airF} and dew point T_{dewF} in °F. These two types of temperature data needed to the weather file base data, but for the equations temperature data are needed in other units. These data, as well as wind speed were obtained from the HMS synoptic station (Szeged) data.

W_{Sadj} is the windspeed data adjusted by the measurement height and the surface roughness (if the wind gauge is at 2 meters, this step is not necessary). The wind gauge of Szeged synoptic station is positioned at a height of 10 meters, but the model calculates with wind speed at 2 meters during the run. To solve this problem, we used a formula in Eq. 1:

$$W_{\text{Sadj}}[\text{m s}^{-1}] = w_{\text{sm}} \cdot (h_{\text{r}} \cdot h_{\text{m}}^{-1})^{\alpha} \quad (1)$$

$$\alpha = 0.12 \cdot z_0 + 0.18$$

where w_{sm} is the measured wind speed, h_{m} is the height of wind measurement, h_{r} is the desired wind speed measurement height, α is an empirical exponent in which z_0 is the roughness height in meter (Davenport et al. 2000).

The liquid precipitation (Precip) and the snow quantity (Snow) are need to be given in m h^{-1} . The model handles separately the two type of precipitation, which gives more accurate results (Yang et al. 2011).

The most complex task within generating the weather file is the calculation of net radiation (Eq. 2):

$$R_{\text{n}}[\text{W m}^{-2}] = S_{\text{n}} + L_{\text{n}} \quad (2)$$

where R_{n} is the net radiation, S_{n} is the net shortwave, and L_{n} is the net longwave radiation. For net shortwave radiation (Eq. 3) the surface albedo is required, which obtained is from the ECMWF ERA Interim database (Berrisford et al. 2011). After the conversion of the available NetCDF files, we made its export in ArcGIS software for 12 and 18 hours within 8-9 days in a month for the area of Szeged. The resulting averages reflect the monthly albedo of the area, which was used to help filter out the outliers.

$$S_{\text{n}}[\text{W m}^{-2}] = (1 - \text{ALB}) \cdot R_{\text{g}} \quad (3)$$

In Eq. 3, the ALB is the average monthly albedo in decimal format, and R_{g} is the global radiation measured at the given time. The net longwave radiation equation contains the following elements:

$$L_{\text{n}}[\text{W m}^{-2}] = \text{ES} \cdot (L_{\text{sky}} + L_{\text{cld}} - L_{\text{sfc}}) \quad (4)$$

where E_S is the surface emissivity for longwave radiation (constant: 0.97), L_{sky} is the downwelling longwave radiation from the sky, L_{cld} is the downwelling longwave radiation from clouds, and L_{sfc} is the upwelling longwave radiation from the surface (Eq. 4).

$$L_{sfc} [W m^{-2}] = \sigma T_{airK}^4 \quad (5)$$

In the L_{sfc} σ is the Stefan-Boltzmann constant ($5.67 \cdot 10^{-8} W m^{-2} K^{-4}$), T_{airK} is the air temperature in K (Eq. 5). The L_{sky} and the L_{cld} consist of the following elements (Eq. 6 and 7):

$$L_{sky} [W m^{-2}] = E \cdot \left(1 - \frac{TOTAL}{10}\right) \cdot \sigma T_{airK}^4 \quad (6)$$

$$L_{cld} [W m^{-2}] = \frac{TOTAL}{10} \cdot \sigma T_{airK}^4 \quad (7)$$

where E is the emissivity of the clear sky, $TOTAL$ is the total current cloud cover in decimal format. In the above equation, the emissivity of the clear sky is an important parameter, if there is no or minimal cloud coverage.

$$E = 0.741 + 0.0062 \cdot T_{dewc} \quad (8)$$

In Eq. 8 T_{dewc} is the dew point in °C (Eq. 8). It can be seen that the temperature data used in the weather file are in English units, while in the equations they are given in SI units, which must be taken into account during processing. However, the key element of the file is the net radiation, which is one of the basic data of the evaporation file.

2.4. Evaporation file

The evaporation file in the model could actually be called potential evaporation and evapotranspiration file. The file is designed to allow Hydro to calculate the actual evaporation rate from actual rate of land cover, depending on potential evaporation data (Wang et al. 2008, Hirabayashi and Endreny 2016, [1]). For this, five different data types need to be created: (potential evapotranspiration from trees), PE (potential evaporation from the ground), PETree (potential evaporation from trees), PESnow (potential evaporation from snow on the ground), and PETreesnow (potential evaporation from snow on tree canopy). It can be clearly seen that, in addition to the evaporation from the liquid precipitate, the model can also take into account the evaporation from the solid precipitate, depending on whether it originates from the canopy or from the surface. As an additional data, the evapotranspiration of the trees is also needed. For calculating the potential evaporation values, a modified Penman-Monteith equation is used (Shuttleworth 1992). The basic data needed for the processing were obtained from the department database (Unger et al. 2017) and from the data of the HMS Synoptic Station.

Basic relations

In order to fill the potential evaporation equations with data, it is necessary to define a few basic relationships and constants. To produce the data of latent heat caused by vaporization (λ) the air temperature (T_{airC}) is required in °C (Eq. 9).

$$\lambda [MJ kg^{-1}] = 2.501 - 0.002361 \cdot T_{airC} \quad (9)$$

The density of water in the air (ρ_w) is necessary to calculate the available water quantity (Eq. 10).

$$\rho_w[\text{kg m}^{-3}] = -0.0051 \cdot T_{\text{airC}}^2 + 0.018 \cdot T_{\text{airC}} + 999.88 \quad (10)$$

Δ is the slope of the vapor pressure temperature curve (Eq. 11):

$$\Delta[\text{kPa } ^\circ\text{C}^{-1}] = \frac{4398e_s}{(237.3+T_{\text{airC}})^2} \quad (11)$$

where e_s is the saturated vapor pressure. The e_s can be calculated from Eq. 12. In addition to the saturated vapor pressure, the vapor pressure is also calculated (e) (Eq. 13).

$$e_s[\text{kPa}] = 0.6108 \exp\left(\frac{17.27 \cdot T_{\text{airC}}}{237.3 + T_{\text{airC}}}\right) \quad (12)$$

$$e[\text{kPa}] = 0.6108 \exp\left(\frac{17.27 \cdot T_{\text{dewC}}}{237.3 + T_{\text{dewC}}}\right) \quad (13)$$

The vapor pressure and the saturated vapor pressure can also be used to calculate the vapor pressure deficit (D) (Eq. 14).

$$D[\text{kPa}] = e_s - e \quad (14)$$

We also need the psychrometric constant (γ) (Eq. 15):

$$\gamma[\text{kPa } ^\circ\text{C}^{-1}] = \frac{C_p \cdot P}{\lambda} \quad (15)$$

where C_p ($=1013 \text{ J kg}^{-1} \text{ } ^\circ\text{C}^{-1}$) is the specific heat of moist air, P (in kPa) is the measured surface pressure.

Wind equations

The potential evaporation and evapotranspiration also strongly depend on the wind conditions, therefore wind speed values, which are projected on the average height of different vegetation types represent a significant factor in the equations. There are several constants in the equations, out of which roughness factors are important. Wind speed varies on the different roughness of the different surfaces, so it is important to define a separate roughness height for each vegetation type:

- The roughness height for water rd_w [m]=0.00137
- The roughness height for trees rd_t [m]=0.95
- The mass transfer coefficient Z_{ov} [m]=0.0123

Since wind measurement at measurement stations is at a given altitude, therefore it is important to assign a height to the different vegetation types, which represents a hypothetical measurement at the height of the vegetation:

- The wind measurement height constant Z_u [m]=2
- The estimated wind measurement height constant for trees Z_{ut} [m]=7
- The estimated wind measurement height constant for the ground Z_{ug} [m]=0.1+ rd_w

After generating the different heights and roughness, the wind speed values for the canopy and the ground can be set. The U_t is the wind speed projected for the tree canopy (Eq. 16), and U_g is the wind speed projected for the ground (Eq. 17):

$$U_t[\text{m s}^{-1}] = U \cdot \frac{\ln\left(\frac{Z_{ut}}{rd_w}\right)}{\ln\left(\frac{Z_u}{rd_w}\right)} \quad (16)$$

$$U_g [\text{m s}^{-1}] = U \cdot \frac{\ln\left(\frac{Z_{ug}}{rd_w}\right)}{\ln\left(\frac{Z_u}{rd_w}\right)} \quad (17)$$

where U is the adjusted wind speed for evaporation, which is calculated in the precipitation file ($W_{S_{adj}}$). (In equation (1) and (16,17) we used different notation for the wind speed ($W_{S_{adj}}/U$ according to the corresponding references because of the easier traceability).

Evaporation equations

The model calculates the potential evapotranspiration of trees (Eq. 18):

$$\text{PET} [\text{m h}^{-1}] = \frac{1}{\lambda \cdot \rho_w} \left[\frac{(\Delta \cdot R_n) + \frac{\rho_a \cdot C_p \cdot D}{r_{a1}}}{\Delta + \gamma \cdot \left(1 + \frac{r_s}{r_{a1}}\right)} \right] \cdot 10^{-3} \quad (18)$$

where r_{a1} is the aerodynamic resistance as described above (Eq. 19), and since transpiration is also investigated, r_s is the stomal resistance (Eq. 20).

$$r_{a1} [\text{s m}^{-1}] = \frac{208}{U_t} \quad (19)$$

$$r_s [\text{s m}^{-1}] = \frac{200}{L} \quad (20)$$

For r_a this simplified formula refers to general vegetation surfaces (such as urban areas), where we do not know the exact composition of vegetation. There is also a plant-specific formula, but for this, it is necessary to have sufficient data on the vegetation of the area. For r_s L denotes the leaf area index (LAI).

It is also necessary to make two aerodynamic resistance values for the calculation of PETree and PE, which are different from those used in the previous equation, as in this case there is no transpiration through the vegetation. The aerodynamic resistance for trees r_{at} (Eq. 21) and the aerodynamic resistance for ground r_{ag} (Eq. 22) are the following:

$$r_{at} [\text{s m}^{-1}] = \frac{4.72 \cdot \left(\ln \frac{Z_{ut}}{Z_{ov} \cdot rd_t}\right)^2}{1 + 0.536 \cdot U_t} \quad (21)$$

$$r_{ag} [\text{s m}^{-1}] = \frac{4.72 \cdot \left(\ln \frac{Z_{ug}}{Z_{ov} \cdot rd_w}\right)^2}{1 + 0.536 \cdot U_g} \quad (22)$$

The PETree is used to calculate evaporation from the surface of the trees (leaf, bark). Thus, this equation does not include the amount of transpiration processes of trees (Eq. 23).

$$\text{PETree} [\text{m h}^{-1}] = \frac{1}{\lambda \cdot \rho_w} \left[\frac{(\Delta \cdot R_n) + \frac{\rho_a \cdot C_p \cdot D}{r_{at}}}{\Delta + \gamma} \right] \cdot 10^{-3} \quad (23)$$

The equation of PE is needed to calculate the amount of water evaporated from the ground of the study site (pervious and impervious surfaces) (Eq. 24).

$$\text{PE} [\text{m h}^{-1}] = \frac{1}{\lambda \cdot \rho_w} \left[\frac{(\Delta \cdot R_n) + \frac{\rho_a \cdot C_p \cdot D}{r_{ag}}}{\Delta + \gamma} \right] \cdot 10^{-3} \quad (24)$$

Since Hydro also handles snow precipitation (Yang et al. 2011), the calculation of evaporation from snow surfaces is also solved. It also consists of two components of the evaporation: evaporation from the canopy and from the ground. In the case of PETreesnow we can calculate the evaporation of snow falling on the canopy (Eq. 25).

$$\text{PETreesnow [m h}^{-1}] = \frac{0.1}{P} \cdot \left\{ \frac{U_t}{\left[\ln\left(\frac{Z_{ut}}{rd_w}\right) \right]^2} \cdot (611.2 - e) \right\} \cdot 10^{-3} \quad (25)$$

For PESnow the potential evaporation of the snow falling on the ground is calculated (Eq. 26).

$$\text{PESnow [m h}^{-1}] = \frac{0.1}{P} \cdot \left\{ \frac{U_g}{\left[\ln\left(\frac{Z_u}{rd_w}\right) \right]^2} \cdot (611.2 - e) \right\} \cdot 10^{-3} \quad (26)$$

After the exact substitution of the equations, we obtain the desired data that Hydro can handle properly. The model works with a comma-delimited file format, so preformatting is necessary.

3. FEASIBLE RESULTS

The Hydro model gives many results, which can help the planners to evaluate the hydrological potential of the vegetation and can be used to draw the attention of decision-makers to the importance of vegetation in urban water management. The model output contains the results in hourly resolution with the help of which, can be analyzed the process and quantity on a given time. The results can be summarized, and these data can show monthly and yearly quantity of processes. The summarized result can be shown the study area hydrological state, and with the help of which can be used to draw the attention of decision-makers the potential water management problem of the study area. If we use the opportunity of modeling different hydrology scenarios, they can be show the consequence of planned greening or square renovation.

The model result can be arrange two main groups. The first main group is the flow results, which can show the quantity of the different flow type. The other main group contains the vegetation processes, and within this, can be distinguish the short vegetation and the tree vegetation type (Table 1).

Table 1 The main result types of the model

Main results	Unit	Main results	Unit
Rainfall	[mm]	Tree canopy evaporation	[m ³ h ⁻¹] [m]
Total runoff	[m ³ h ⁻¹]	Tree canopy throughfall	[m ³ h ⁻¹] [m]
Baseflow	[m ³ h ⁻¹]	Tree canopy storage	[m ³ h ⁻¹] [m]
Flow on pervious surface	[m ³ h ⁻¹]	Precipitation on short vegetation	[m ³ h ⁻¹] [m]
Flow on impervious surface	[m ³ h ⁻¹]	Short vegetation interception	[m ³ h ⁻¹] [m]
Infiltration	[m ³ h ⁻¹] [m]	Short vegetation evaporation	[m ³ h ⁻¹] [m]
Precipitation on tree canopy	[m ³ h ⁻¹] [m]	Short vegetation throughfall	[m ³ h ⁻¹] [m]
Tree canopy interception	[m ³ h ⁻¹] [m]	Short vegetation storage	[m ³ h ⁻¹] [m]

As the Fig. 4 shows, the model gives comprehensive picture about the flow and the processes of the vegetation on the study site. Based on these results, we can provide

information about a whole year hydrological state and the vegetation contribution to the runoff reduction. The quantitative data can provide a good basis for the urban planning documents.

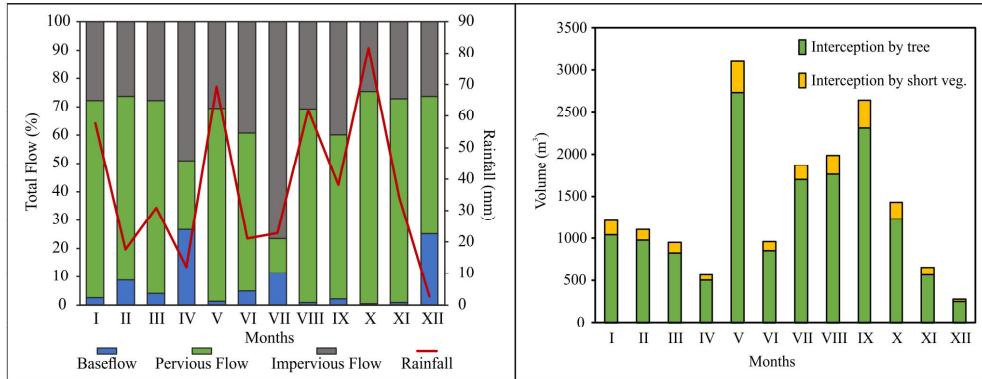


Fig. 4 Sample flow and interception results of Hydro

4. CONCLUSION

The advantage of the UFORE-Hydro model compared to other available hydrology and stormwater management models is the high consideration of vegetation surfaces (Kirnbauer et al. 2013, Jayasooriya and Ng 2014, Nowak et al. 2018). However, in the study of meteorological and hydrological processes, due to their complexity, there is a great chance for error. Complexity is further enhanced by the consideration of different vegetation surfaces, thereby the chance of error also increases. Therefore, it is important that the input files of the model are based on accurate databases. The required files have been created in the US so far (with some basic data), but the additional data came from databases with low geometric resolution. For the regular and high-precision use of the model in Hungary, it is necessary that the files are based on entirely Hungarian databases and files built by individual users. In this paper, we made a step-by-step introduction guide of the structure of the input files from the basics and the available databases for their production. We listed the databases that can be used to generate the files. At national level, few cities have a measuring network density such as Szeged (Unger et al. 2017); in their case, the HMS and SYNOP databases can serve as appropriate bases. For the albedo we used the free database of ECMWF ERA Interim (Berrisford et al. 2011), which available for everyone. The leaf surface index can be obtained either by field measurements or from literature and modeled data. After obtaining the data, it is important to load the equations accurately, as several other equations (e.g. R_n) are based on each basic equation.

With these steps, the UFORE-Hydro's adaptation in Hungary is feasible from the point of view of meteorological data. The refinement of the databases is naturally desirable, but the requirements of the model input parameter can be done with these solutions. By using Hydro, we can obtain a picture of the current hydrology processes in the study sites, but as we have the ability to run scenarios, it can also be used in urban planning. Research on a small study site can contribute to a whole city level research. As a result of our adaptation,

the input data comes from a reliable, accurate source, and can be extended to a significant part of Hungarian cities.

REFERENCES

- Balázs B, Unger J, Gál T, Sümeghy Z, Geiger J, Szegedi S (2009) Simulation of the mean urban heat island using 2D surface parameters: empirical modeling, verification and extension. *Meteorol Appl* 16:275-287
- Baatz M, Schape A (2000) Multiresolution Segmentation: an optimization approach for high quality multi-scale image segmentation. In: Strobl J, Blaschke T, Griesbner G (eds) *Angewandte Geographische Informationsverarbeitung*, Vol. 12. Wichmann-Verlag, Heidelberg, 12-23
- Berrisford P, Dee DP, Poli P, Brugge R, Fielding M, Fuentes M, Kállberg PW, Kobayashi S, Uppala S, Simmons A (2011) The ERA-Interim archive Version 2.0. ERA Report, 23 p.
- Berland A, Shiflett SA, Shuster WD, Garmestani AS, Goddard HC, Herrmann DL, Hopton ME (2017) The role of trees in urban stormwater management. *Landscape Urban Plan* 162:167-177
- Buzás K (ed) (2012) *Települési csapadékvíz-gazdálkodás*. [Urban stormwater management. (in Hungarian)] TERC Kereskedelmi és Szolgáltató Kft, Budapest
- Davenport AG, Grimmond CSB, Oke TR, Wieringa J (2000) Estimating the roughness of cities and sheltered country. Proc. 12th Conf. Applied Climatology, Am. Meteorol. Soc., Boston, 96-99
- Department of Water (2007) *Stormwater Management Manual for Western Australia*. Department of Water 2004-2007
- Fletcher TD, Shuster W, Hunt WF, Ashley R, Butler D, Arthur S, Trowsdale S, Barraud S, Semadeni-Davies A, Bertrand-Krajewski JL, Mikkelsen PS, Rivard G, Uhl M, Dagenais D, Viklander M (2015) SUDS, LID, BMPs, WSUD and more – The evolution and application of terminology surrounding urban drainage. *Urban Water J* 12:525-542
- Gayer J, Ligetvári F (2007) *Települési vízgazdálkodás, csapadékvíz elhelyezés*. [Urban stormwater management, stormwater disposal. (in Hungarian)] Környezetvédelmi és Vízügyi Minisztérium, Budapest
- Hay GJ, Castilla G, Wulder MA, Ruiz JR (2005) An automated object-based approach for the multiscale image segmentation of forests scenes. *Int J Appl Earth Obs* 7(4):339-359
- Hirabayashi S, Endreny TA (2016) Surface and upper weather pre-processor for i-Tree Eco and Hydro. i-Tree Eco and UFORE Resources, Version 1.2, 19 p.
- Jayasooriya VM, Ng AWM (2014) Tools for modeling of stormwater management and economics of green infrastructure practices: A review. *Water Air Soil Pollut* 225:2055-2075
- Kimbauer MC, Baetz BW, Kenney WA (2013) Estimating the stormwater attenuation benefits derived from planting four monoculture species of deciduous trees on vacant and underutilized urban land parcels. *Urban For Urban Gree* 12(3):401-407
- Kiss M, Takács Á, Pogácsás R, Gulyás Á (2015) The role of ecosystem services in climate and air quality in urban areas: Evaluating carbon sequestration and air pollution removal by street and park trees in Szeged (Hungary). *Morav Geogr Rep* 23(3):36-46
- Liu CM, Chen JW, Hsieh YS, Liou ML, Chen TH (2015) Build Sponge Eco-cities to Adapt Hydroclimatic Hazards. In: Leal Filho W (eds) *Handbook of Climate Change Adaptation*. Springer, Berlin, Heidelberg
- Manakos I, Schneider T, Ammer U (2000) A comparison between the isodata and the eCognition classification methods on basis of field data. *ISPRS 2000*, Vol. XXXIII, Supplement CD, Amsterdam
- Mucsi L, Kovács F, Henits L, Tobak Z, van Leeuwen B, Szatmári J, Mészáros M (2007) Városi területhasználat és felszínborítás vizsgálata távérzékeléses módszerekkel. In: Mezősi G (szerk) *Városökológia* [Examination of urban land use and land cover by remote sensing. In: Mezősi G (eds) *Urban ecology* (in Hungarian)] *Földrajzi Tanulmányok* 1:43-65
- Nowak DJ, Maco S, Binkley M (2018) i-Tree: Global tools to assess tree benefits and risks to improve forest management. *ASCA Arbor Consult* 51(4):10-13
- Raymond CM, Berry P, Breil M, Nita MR, Kabisch N, de Bel M, Enzi V, Frantzeskaki N, Geneletti D, Cardinaletti M, Lovinger L, Basnou C, Monteiro A, Robrecht H, Sgrigna G, Munari L, Calfapietra C (2017) An impact evaluation framework to support planning and evaluation of Nature-based solutions projects. Report prepared by the EKLIPSE Expert Working Group on Nature-based Solutions to Promote Climate Resilience in Urban Areas. Centre for Ecology & Hydrology
- Romnée A, Evrard A, Trachte S (2015) Methodology for a stormwater sensitive urban watershed design. *J Hydrol* 530:87-102

Adaptation of UFORE-Hydro model for Szeged and the southern region of the Great Hungarian Plain based on local meteorological database

- Shuttleworth WJ (1992) Evaporation. In: Maidment D (ed) Handbook of hydrology. McGraw Hill: New York, NY, USA.
- Unger J, Lelovics E, Gál T (2014a) Local Climate Zone mapping using GIS methods in Szeged. *Hun Geo Bull* 63(1):29-41
- Unger J, Lelovics E, Gál T, Mucsi L (2014b) A városi hősziget fogalom finomítása a lokális klímazónák koncepciójának felhasználásával – példák Szegedről. [Refining the concept of urban heat island using the concept of local climate zones – examples from Szeged. (in Hungarian)] *Földrajzi Közlemények* 138(1):50-63
- Unger J, Gál T (2017) Városklíma. [Urban Climate (in Hungarian)] Szeged, GeoLitera, 256 p.
- Unger J, Skarbit N, Gál T (2017) Szegedi városklíma mérőállomás-hálózat és információs rendszer. [Urban climate measurement station network and information system of Szeged. (in Hungarian)] *Léggör* 62(3):114-118
- UN DESA [United Nations, Department of Economic and Social Affairs, Population Division] (2019) World Urbanization Prospects: The 2018 Revision (ST/ESA/SER.A/420). New York, United Nations
- US EPA [US Environmental Protection Agency] (2003) Protecting Water Quality from Urban Runoff. EPA 841-F-03-003
- Wang J, Endreny TA, Nowak DJ (2008) Mechanistic simulation of tree effects in an urban water balance model. *J Am Water Resour Assoc* 44(1):75-84
- Xiao Q, McPherson EG (2002) Rainfall interception by Santa Monica's municipal urban forest. *Urban Ecosyst* 6:291-302
- Yang Y, Endreny TA, Nowak DJ (2011) iTree-Hydro: Snow hydrology update for the Urban Forest Hydrology Model. *J Am Water Resour Assoc* 47(6):1211-1218
- [1] i-Tree Hydro User's Manual v5.1. (2016) (https://www.itreetools.org/documents/241/Hydro_Manual_v5.1.pdf)
- [2] Melbourne Water Introduction to WSUD (<https://www.melbournewater.com.au/planning-and-building/stormwater-management/introduction-wsud>)

PROJECTION OF PRESENT AND FUTURE DAILY AND EVENING URBAN HEAT LOAD PATTERNS

J UNGER, N SKARBIT and T GÁL

*Department of Climatology and Landscape Ecology, University of Szeged, Egyetem u. 2., 6720 Szeged, Hungary,
E-mail: unger@geo.u-szeged.hu*

Summary: In this modeling study the recent and future daily and evening thermal climate of a Central-European city (Szeged, Hungary) was investigated in terms of heat load modification by applying MUKLIMO_3 model to project daily and evening climate indices. For surface parameterization the Local Climate Zone (LCZ) scheme was used. The investigation encompassed three climatological time periods (1981–2010, 2021–2050 and 2071–2100) and two emission scenarios for future climate (RCP4.5 and RCP8.5). Our results show that highest index values appear in the city centre and stretch to the NW direction (LCZs 2, 3 and 8) and they decrease towards the vegetated rural surfaces (mainly LCZ D). That is, the values depend on the zone types and there are more days towards the densely built-up LCZs. Also, a general temporal change can be detected as the index patterns show the substantial increasing tendency for both indices towards the end of this century. This temporal change suggests a two-way conclusion: first, the increasing number of hot days means a strongly deteriorating change of unfavourable thermal conditions, and second, the change in the number of the evening index provides more opportunities for regeneration and leisure-time activities outdoors in the already thermally less stressful evening hours for the urban inhabitants. This study gives very illustrative examples on the expected climate changes during this century and these examples show that there are several sides to these changes in urban environments. Furthermore, they clearly prove that global or regional scale climate predictions without urban climate interactions do not have enough detailed information.

Key words: urban heat load, climate indices, present, future scenarios, Central Europe

1. INTRODUCTION

Research on urban climate is focused on different climate modifications caused by the built environments, in addition it also attempts to provide reliable projections for future climatic situations at local scale. Urban population follows a rapidly growing trend (UN 2019) which underlines the importance of the role of urban climate research. In order to reveal the effects of regional to local scale atmospheric phenomena, Regional Climate Models (RCM) are applied. This type of models is nested into General Circulation Models (GCM) whose output data serve as boundary conditions for the RCMs (McGregor 1997). To predict future climate patterns it is necessary to expect different possible future anthropogenic activity trends, therefore, the model runs are combined with future emission scenarios. In recent years there are four scenarios called them as Representative Concentration Pathways (RCP) distinguished by the enhanced radiative forcings resulting from different predicted levels of greenhouse gas concentrations (Stocker et al. 2014).

To simulate these modified climatological processes in urban areas via numerical models the spatial resolution of the models should be able to reflect the urban effects and the varied urban surfaces need to be differentiated from natural landscapes (Oke et al. 2017). MUKLIMO_3 (Sievers 1995), ENVI-met (Bruse and Fleer 1998) and Town Energy Balance

models (Masson 2000) as specific urban climate models (UCM) are the most accurate approaches for urban climate modelling (Hidalgo et al. 2008).

To reveal the joint effects of climate change and urban areas, both the RCMs and UCMs are needed as they are able to deliver climate data on a regional scale and provide the climate modification by cities, respectively. One of the several approaches for surface parameterizations reflecting the effects of different surface units is the Local Climate Zone (LCZ) scheme. It is a climate-based classification system categorizing the different land-use areas by objectively quantified measures, that is, each zone is defined by its own geometric, surface cover, thermal and radiative properties (Stewart and Oke 2012). Therefore, this scheme can be used for surface input data for numerical modeling (Žuvela-Aloise 2017, Kwok et al. 2019).

As the settlements have an additional temperature-rising effect, the so-called urban heat island (UHI) phenomenon, the inhabitants of the strongly built-up and therefore less vegetated cities suffer from this excess heat load more than their counterparts living in the generally greener countryside, especially in heat wave periods (Hatvani-Kovacs et al. 2018, Hintz et al. 2018). As the UHI is mostly pronounced in the nocturnal hours, this thermal excess can be particularly dangerous at night causing, for example, higher mortality rate (McGregor et al. 2015).

The paper focuses on the recent and future daily and evening thermal climate of a Central-European city (Szeged, Hungary) by applying the MUKLIMO_3 microclimatic numerical model (Sievers 1995). In the region of Szeged a warming trend can be anticipated during the next decades (Skarbit and Gál 2016, Bokwa et al. 2018, 2019). The main purpose of this study is to analyze and compare the patterns of the annual numbers of daily and evening climate indices in the present (1981–2010) and in the periods of future climate change (2021–2050 and 2071–2100) based on a relatively optimistic future emission scenario (RCP4.5) and a much more pessimistic one (RCP8.5).

2. STUDY AREA, DATA AND METHODS

2.1. Study area and its land-use classes

Szeged (46.3°N, 20.1°E) is located in a flat terrain of south-eastern Hungary at about 80 m above sea level (Fig. 1). Its region belongs to the Köppen's climatic class of Cfa (temperate, no dry season, hot summer) (Köppen 1918, Unger et al. 2020). The city has 162,000 inhabitants and contains a densely and midlevel height built centre, openly arranged blocks of flats, large areas of family houses as well as shopping centers and warehouses. The rural areas around the city are mostly arable lands (e.g. maze) but in some places they are interrupted by groves (Skarbit et al. 2017). The presented climatic parameters of Szeged region (Table 1) are based on CRU TS v4.03 database (Harris et al. 2014).

The LCZ map of Szeged has a spatial resolution of 100 m (Fig. 1). The city centre mainly consists of LCZs 2 and 3 (compact midrise and compact low-rise). Open midrise (LCZ 5) can be found north, northeast and south from the centre. LCZs 6 and 9 (open low-rise and sparsely built) occupies a large area south, north and northeast in the suburbs. LCZ 8 (large low-rise) covers a relatively large area in the northwest. Around the urbanized districts the prevailing land-use types are low plants (LCZ D).

These LCZ classes were used as input land-use data for the MUKLIMO_3 simulations (see Section 2.2).

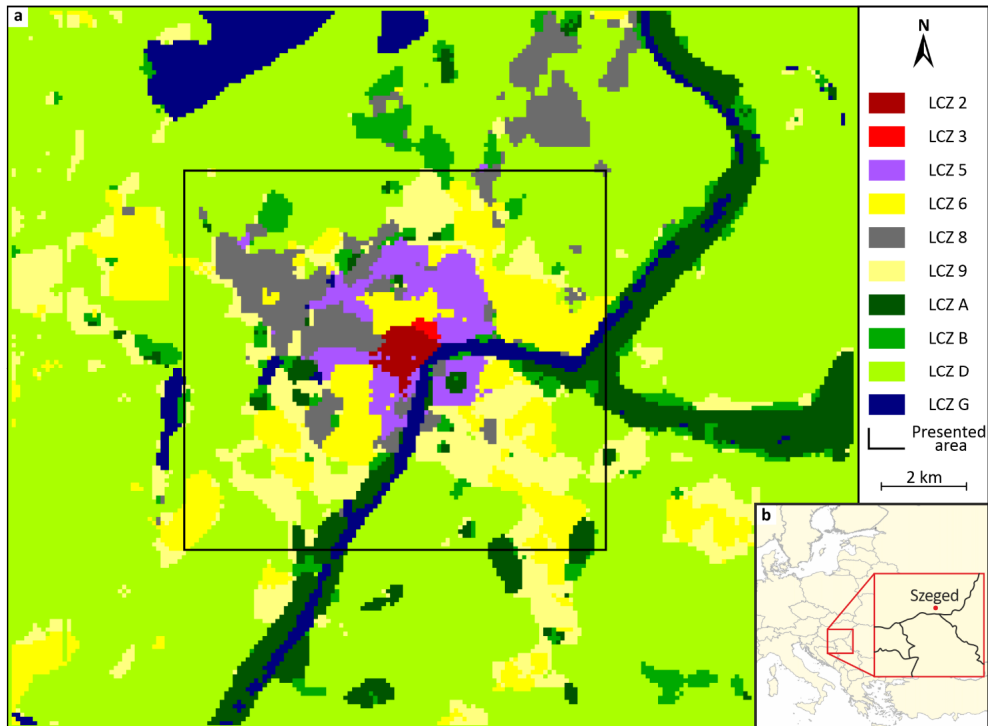


Fig. 1 Land-use class map in and around Szeged based on the LCZ classification system (the study area is indicated by black frame) (Skarbit and Gál 2016)

Table 1 Main climatic parameters (1986–2015) of Szeged region (Harris et al. 2014)

Mean annual temperature	11.9°C
Highest mean monthly temperature (July)	22.7°C
Lowest mean monthly temperature (January)	0.4°C
Mean annual amount of precipitation	508 mm

2.2. Urban climate modelling, climate indices

The model simulations at urban scale for this study were carried out with the non-hydrostatic microclimatic MUKLIMO_3 model (Sievers 1995). For more details about the model see Früh et al. (2011a), Skarbit and Gál (2016) and Žuvela-Aloise (2017).

For calculating climate indices the model needs climate input data. In this study results from global and regional climate projections were used as input data (air temperature, relative humidity, wind speed and direction) from the EURO-CORDEX projections (Jacob et al. 2014) with 0.11° spatial resolution (5 different GCMs and 3 different RCMs resulting 14 different simulations based on RCP4.5 and RCP8.5 scenarios). For the details about the applied models see Gál et al. (2021).

The cuboid method was applied which is a practical interpolation technique including meteorological data for a 30-year period without enormous computational efforts (Früh et al.

2011a). In the case of urban heat load, it is assumed that only the 2-m air temperature (T), the 2-m relative humidity and the 10-m wind velocity are the contributing factors.

In this study, the annual numbers of hot days and beergarden days were considered as climate indices measuring the urban heat load in the daytime and evening, respectively (Früh et al. 2011b, Skarbit and Gál 2016). The definition of the hot day is when the daily T_{max} equals or exceeds 30°C. A beergarden day is a day when the T is at least 20°C at 20h (LST), that is evenings people can sit in the open (in beergardens, restaurants, caffes, open-air theatres etc.) at that time without feeling cold. These evenings are important from the point of view of leisure-time quality in climatic zones characterized by a longer cold season. The patterns of the index numbers were calculated both for the present and for the future for all scenarios. The northwest and northeast directions were selected as prevailing wind directions for the Szeged region (based on the data of nearby WMO station 12982).

3. RESULTS AND DISCUSSION

3.1. Present heat load patterns

Simulated patterns for the present (1981–2010) can be followed on Fig. 2. In this period the number of hot days exceeds 30 in the city centre (Fig. 2a). Close to the centre (LCZs 2 and 3) and both in the northern (LCZ 5) and in the northwestern parts of the city (LCZ 8) there are 20-25 hot days per a year, while in the suburbs (LCZs 6 and 9) there are only 10 to 20. In the large urban parks and green areas the values are below 10.

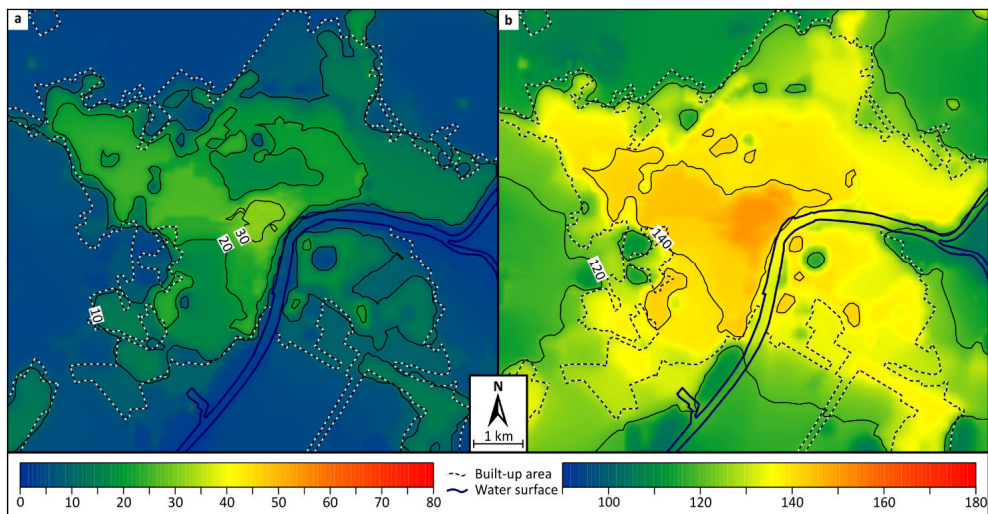


Fig. 2 Patterns of the annual number of hot days (a) and beergarden days (b) in the present (1981–2010) (the boundary of the built-up area is indicated by white-black dashed line)

The spatial distribution of the evening index in the present shows a bit similar pattern (Fig. 2b). In the central areas (LCZs 2 and 3) the number of the beergarden days exceeds 150, and the area of more than 140 extends NW following the industrial and warehouse zones

(LCZ 8), as well as southwards (LCZ 5). In the suburbs (LCZs 6 and 9) this index is still over 120 while in the surrounding rural areas (mainly LCZ D) its number is between 100 and 120.

3.2. Future heat load patterns

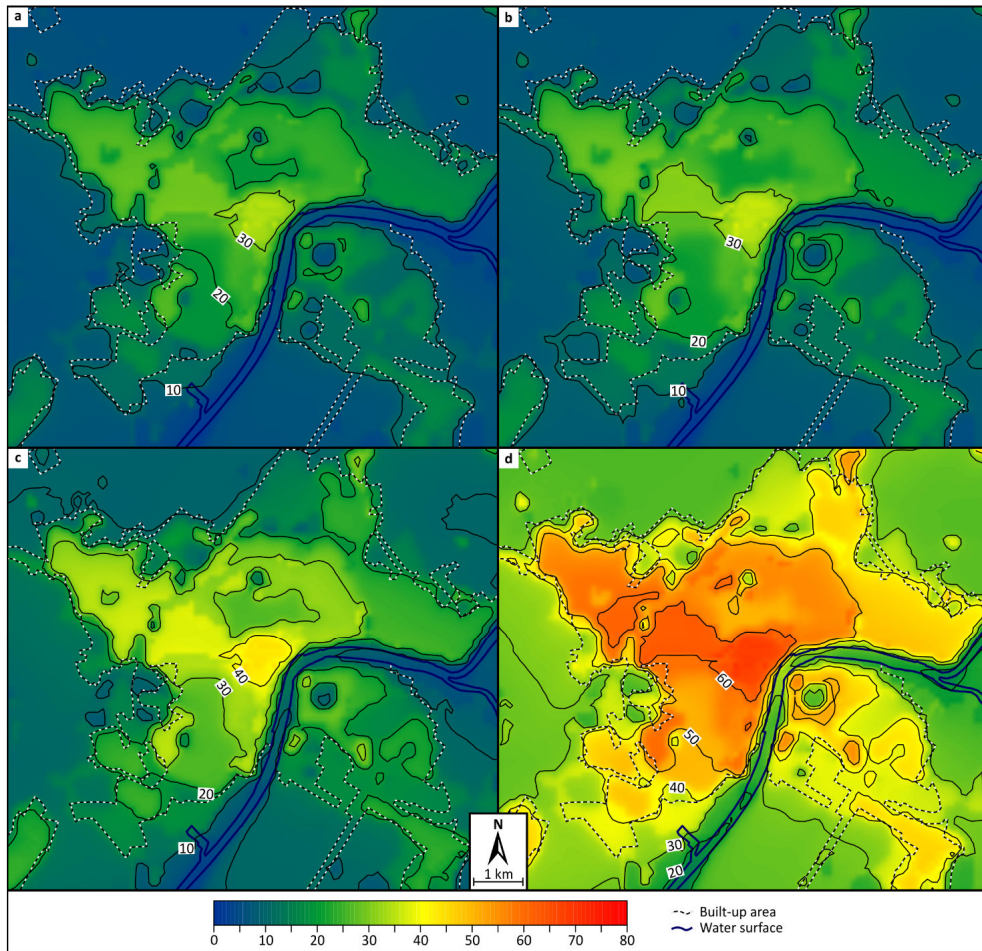


Fig. 3 Patterns of the annual number of hot days in the periods of 2021–2050 (a, b) and 2071–2100 (c, d) based on RCP4.5 (a, c) and RCP8.5 (b, d)

Fig. 3 shows the patterns of the number of hot days for two future periods (2021–2050 and 2071–2100) based on RCP4.5 and RCP8.5 scenarios. In the period of 2021–2050 (Figs. 3a-b), the difference in the patterns between the two scenarios is not very significant: in the city centre (LCZs 2 and 3) the number is around 30-35 although this area is larger in the case of RCP8.5 as it covers some parts of LCZ 8 towards NW. The area of 20-30 is much more extensive as stretches towards NW (LCZ 8), northwards and southwards (LCZ 5). In the case of RCP8.5 the 20-day isoline extends a bit towards the SW (LCZ 6). It can also be seen that

in the urban parks this index value remains below 10. In the surrounding rural areas (mainly LCZ D) the annual number of hot days is also smaller than 10.

Based on the results of 2071–2100, the emission scenarios deliver two distinct outcomes (Figs. 3c and 3d). When the emissions decline at the end of the century (RCP4.5) (Fig. 3c), the further warming is slight comparing to the period of 2021–2050 (Fig. 3a). The city centre (LCZs 2 and 3) has an additional number of about 10 (40–45 hot days a year). Close to the centre there are 30–40 hot days with a larger area of 20–30 stretching towards NW, while in the suburbs (LCZs 6 and 9) their numbers are still over 20 days. Urban green spaces and rural areas remain cool in this case (hot days less than 10).

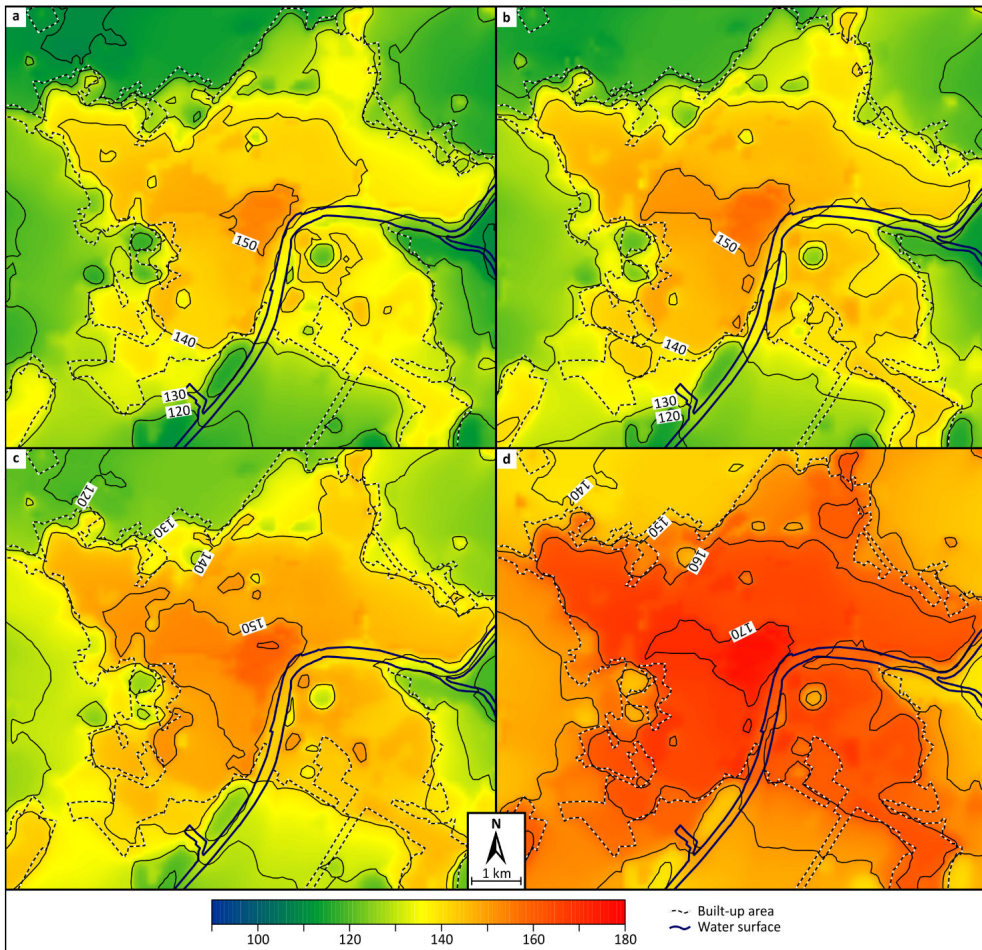


Fig. 4 Annual number of beergarden days in the periods of 2021–2050 (a, b) and 2071–2100 (c, d) based on RCP4.5 (a, c) and RCP8.5 (b, d)

In the case of the pessimistic scenario (RCP 8.5) the daily heat load drastically increases in the whole domain (Fig. 3d). In the city centre and NW to it (LCZs 2, 3 and 8) the number of hot days exceeds 60 a year which is a 30-day rise compared to the earlier

periods (Figs. 2b and 3b). In addition, almost the entire built-up area experiences more than 40 hot days. Even the surrounding rural areas (mainly LCZ D) has the index number of about 20. Like cool islands, the larger city parks experience a relatively smaller levels of heat load (20-30 hot days).

The number of pleasant evenings (beergarden days) in the future periods can be followed by Fig. 4. In the period of 2021–2050 (Figs. 4a and 4b), the difference in the patterns between the two scenarios is minor: in the city centre (LCZs 2 and 3) the number is over 150 although this area is larger in the case of RCP8.5 as it covers some parts of LCZ 8 towards NW. The area of over 140 is much more extensive stretching towards NW (LCZ 8), northwards and southwards (LCZ 5), moreover, in the case of RCP8.5, also to the east (LCZ 6) and the SE (LCZs 6 and 9) (Fig. 4b). In the urban parks this evening index value remains below 120 and in the rural areas the values are between 120 and 130.

In the period at the end of the century, according to the favorable scenario, the number of beergarden days in the wider central areas (LCZs 2, 3 and 8) is over 150, moreover, even in a limited downtown area, it even exceeds 160. The isoline of 140 surrounding the interiors in the present period (Fig. 2b) now practically frames the entire urban area (Fig. 4c). By this time, the city parks and the rural areas near the suburbs can be characterized by index values of 130-140, and they fall below 130 only further away from the built-up parts.

In the case of RCP 8.5 the evening measure drastically increases both in the urbanized and rural areas (Fig. 4d). In the city centre and NW of it (LCZs 2, 3 and 8) its values exceeds 170 rising 20-30 days compared to the earlier periods (Figs. 2b and 4b). In most parts of the city the index value is above 160, but it is above 150 even in the suburbs. The urban green spaces and the rural areas can also be characterized by the pleasant evenings of at least 140.

4. CONCLUSIONS

In this paper a modelling study was presented by applying the MUKLIMO_3 urban model (Sievers 1995) in order to project the recent and future daily and evening thermal climate of a Central-European city (Szeged, Hungary). The model is able to reveal the microscale climatic effects of different of land-use types, namely the thermal effect of the elements of the LCZ scheme (Stewart and Oke 2012). This study intended to highlight the joint thermal effects of urban climate and global climate change. Our main purpose was to analyze and compare the annual patterns of the daily and evening climate index values in the present (1981–2010) and in the periods of future climate change (2021–2050 and 2071–2100) based on optimistic (RCP4.5) and pessimistic (RCP8.5) future emission scenarios.

According to the obtained patterns the areas with the largest index values appear in the city centre extended NW to it (LCZs 2, 3 and 8) as well as the values decrease towards to the vegetated rural surfaces (LCZ D). That is, the values depend on the zone types and there are more days towards to the densely built-up LCZs. Additionally, a general temporal change can be detected as the index patterns show the substantial increasing tendency for both indices towards the end of this century. Table 2 helps to summarize the main trends in the change that are expected in the future. It contains the change in the numbers (rounded to ten) of the hot and beergarden days in the city centre between the recent (1981–2010) and future simulated cases (2021–2050 and 2071–2100), as well as the differences between the rural and central areas.

Table 2 Increase of the hot and beergarden days in the city centre (LCZ 2) between the recent (1981–2010) and future simulated cases (2021–2050 and 2071–2100) based on the RCP4.5 and RCP8.5 scenarios, as well as the differences (in paranthesis) between the rural (LCZ D) and centre (LCZ 2) areas (the numbers are rounded to ten)

Climate index	Present period 1981–2010	Scenario	Future periods	
			2021–2050	2071–2100
hot days	0 (30)	RCP4.5	0 (30)	10 (40)
		RCP8.5	0 (40)	30 (50)
beergarden days	0 (30)	RCP4.5	10 (40)	10 (40)
		RCP8.5	20 (50)	30 (40)

As Table 2 shows, the change in the period of 2021–2050 compared to the reference period and the difference between the two scenarios is slight, although in the case of the evening index the increase is twice as large for scenario RCP8.5 (20 days) as for the optimist one. In contrary, in the distant future the increase is more significant and the two scenarios project different patterns in terms of the index value magnitudes.

However, drawing conclusions from these temporal changes in the index values in an urban environment points in two directions:

(i) On the one hand, the increasing number of hot days expresses a strongly deteriorating change in unfavourable and stressful thermal conditions until the end of the century.

(ii) On the other hand, the change in the number of the evening index can actually be considered a positive development, as it provides more opportunities for regeneration and leisure-time activities outdoors in the already thermally less stressful evening hours for the urban inhabitants.

The obtained results are very illustrative examples for the demonstration of the expected changes of the climate during this century and these examples show that there are several sides to these changes in urban environments. Furthermore, they clearly prove that global or regional scale climate predictions without urban climate interactions do not have enough detailed information for urban planners or local authorities.

Acknowledgement: This research has been supported by the National Research, Development and Innovation Office, Hungary (NKFI K-120346).

REFERENCES

- Bokwa A, Dobrovolný P, Gál T, Geletiĉ J, Gulyás Á, Hajto MJ, Holec J, Hollósi B, Kielar R, Lehnert M, Skarbit N, Šťastný P, Švec M, Unger J, Walawender JP, Žuvela-Aloise M (2018) Urban climate in Central European cities and global climate change. *Acta Climatol* 51-52:7-35
- Bokwa A, Geletiĉ J, Lehnert M, Žuvela-Aloise M, Hollósi B, Gál T, Skarbit N, Dobrovolný P, Hajto M J, Kielar R, Walawender J P, Šťastný P, Holec J, Ostapowicz K, Burianová J, Garaj M (2019) Heat load assessment in Central European cities using an urban climate model and observational monitoring data. *Energ Buildings* 201:53-69
- Bruse M, Fler H (1998) Simulating surface–plant–air interactions inside urban environments with a three dimensional numerical model. *Environ Mod Softw* 13:373-384
- Früh B, Becker P, Deutschländer T, Hessel JD, Kossmann M, Mieskes I, Namyslo J, Roos M, Sievers U, Steigerwald T, Turau H, Wienert U (2011a) Estimation of climate-change impacts on the urban heat load using an urban climate model and regional climate projections. *J Appl Meteorol Clim* 50:167-184

- Früh B, Kossmann M, Roos M (2011b) Frankfurt am Main im Klimawandel – Eine Untersuchung zur städtischen Wärmebelastung. Berichte des Deutschen Wetterdienstes 237. Offenbach am Main, Selbstverlag des Deutschen Wetterdienstes, Offenbach am Main, 68 p.
- Gál T, Mahó SI, Skarbit N, Unger J (2021) Analysis of the effect of different urban green spaces on urban heat load patterns in the present and in the future. *Comput Environ Urban* (accepted)
- Harris I, Jones PD, Osborn TJ, Lister DH (2014) Updated high-resolution grids of monthly climatic observations – the CRU TS3.10 Dataset. *Int J Climatol* 34:623-642
- Hatvani-Kovacs G, Bush J, Sharifi E, Boland J (2018) Policy recommendations to increase urban heat stress resilience. *Urban Clim* 25:51-63
- Hidalgo J, Masson V, Baklanov A, Pigeon G, Gimeno L (2008) Advances in urban climate modelling. *Ann NY Acad Sci* 1146:354-374
- Hintz MJ, Luederitz C, Lang DJ, von Wehrden H (2018) Facing the heat: A systematic literature review exploring the transferability of solutions to cope with urban heat waves. *Urban Clim* 24:714-727
- Jacob D, Petersen J, Eggert B, Alias A, Christensen OB, Bouwer LM, Braun A, Colette A, Déqué M, Georgievski G, Georgopoulou E (2014) EURO-CORDEX: new high-resolution climate change projections for European impact research. *Reg Environ Change* 14:563-578
- Köppen W (1918) Klassifikation der Klimate nach Temperatur, Niederschlag und Jahreslauf. *Pettersman Geogr Mitteilungen* September/Oktoberheft:194-203
- Kwok YT, Schoetter R, Lau KK-L, Hidalgo J, Ren C, Pigeon G, Masson V (2019) How well does the local climate zone scheme discern the thermal environment of Toulouse (France)? An analysis using numerical simulation data. *Int J Climatol* 39:5292-5315
- Masson V (2000) A physically-based scheme for the urban energy budget in atmospheric models. *Bound-Lay Meteorol* 94:357-397
- McGregor JL (1997) Regional climate modelling. *Meteorol Atmos Physics* 63:105-117
- McGregor GR, Bessemoulin P, Ebi K, Menne B (eds) (2015) *Heatwaves and Health: Guidance on Warning-System Development*. WMO-No. 1142, World Meteorological Organization – World Health Organization, ISBN 978-92-63-11142-5, 96 p.
- Oke TR, Mills G, Christen A, Voogt JA (2017) *Urban Climates*. Cambridge University Press, Cambridge, 523 p.
- Sievers U (1995) Verallgemeinerung der Stromfunktionsmethode auf drei Dimensionen. *Meteorol Zeitschrift* 4:3-15
- Skarbit N, Gál T (2016) Projection of intra-urban modification of night-time climate indices during the 21st century. *Hung Geogr Bull* 65:181-193
- Skarbit N, Stewart ID, Unger J, Gál T (2017) Employing an urban meteorological network to monitor air temperature conditions in the ‘local climate zones’ of Szeged (Hungary). *Int J Climatol* 37/S1:582-596
- Stewart ID, Oke TR (2012) Local climate zones for urban temperature studies. *Bull Am Meteorol Soc* 93:1879-1900
- Stocker TF, Qin D, Plattner G-K, Tignor M, Allen SK, Boschung J, Nauels A, Xia Y, Bex V, Midgley PM (2013) *Climate Change 2013: The Physical Science Basis. Contribution of Working Group I to the Fifth Assessment Report of the Intergovernmental Panel on Climate Change*. Cambridge University Press, Cambridge, United Kingdom and New York, NY, USA
- United Nations, Department of Economic and Social Affairs, Population Division (2019) *World Urbanization Prospects: The 2018 Revision (ST/ESA/SER.A/420)*. New York, United Nations
- Unger J, Skarbit N, Kovács A, Gál T (2020) Comparison of regional and urban outdoor thermal stress conditions in heatwave and normal summer periods: A case study. *Urban Clim* 32:100619
- Žuvela-Aloise M (2017) Enhancement of urban heat load through social inequalities on an example of a fictional city King’s Landing. *Int J Biometeorol* 61:527-539

MODEL DEVELOPMENT FOR THE ESTIMATION OF URBAN AIR TEMPERATURE BASED ON SURFACE TEMPERATURE AND NDVI – A CASE STUDY IN SZEGED

Y GUO¹, T GÁL¹, G TIAN², H LI^{2,3} and J UNGER¹

¹*Department of Climatology and Landscape Ecology, University of Szeged, Egyetem u. 2., 6720 Szeged, Hungary
E-mail: guoyuchen@geo.u-szeged.hu*

²*College of Landscape Architecture and Art, Henan Agricultural University, Nongye str. 63., 450002 Zhengzhou, China*

³*Department of Landscape Planning and Regional Development, Szent István University, Villányi u. 29-43., 1118 Budapest, Hungary*

Summary: Predictive models for urban air temperature (T_{air}) were developed by using urban land surface temperature (LST) retrieved from Landsat-8 and MODIS data, NDVI retrieved from Landsat-8 data and T_{air} measured by 24 climatological stations in Szeged. The investigation focused on summer period (June–September) during 2016–2019 in Szeged. The relationship between T_{air} and LST was analyzed by calculating Pearson correlation coefficient, root-mean-square error and mean-absolute error using the data of 2017–2019, then unary (LST) and binary (LST and NDVI) linear regression models were developed for estimating T_{air} . The data in 2016 were used to validate the accuracy of the models. Correlation analysis indicated that there were strong correlations during the nighttime and relatively weaker ones during the daytime. The errors between T_{air} and $LST_{\text{MODIS-Night}}$ was the smallest, followed by $LST_{\text{MODIS-Day}}$ and $LST_{\text{Landsat-8}}$ respectively. The validation results showed that all models could perform well, especially during nighttime with an error of less than 1.5°C. However, the addition of NDVI into the linear regression models did not significantly improve the accuracy of the models, and even had a negative effect. Finally, the influencing factors and temporal and spatial variability of the correlation between T_{air} and LST were analyzed. $LST_{\text{Landsat-8}}$ had a larger original error with T_{air} , but the regression model based on Landsat-8 had a stronger ability to reduce errors.

Key words: Surface temperature, air temperature, NDVI, correlation and error analysis, predictive model, Szeged

1. INTRODUCTION

Urbanization is characterized by extensive land use transformation and altered surface thermal characteristics (Kalnay and Cai 2003, Shiflet et al. 2017). By changing the material and energy flows, urbanization has transformed the natural ecosystem to a coupled human and natural system, which inevitably has resulted in various effects on the eco-environment, including effects on the urban thermal environment, especially in urban regions having intensive population and high building density (Peng et al. 2016). One representative effect on the urban thermal environment is the appearance of urban heat island (UHI), a phenomenon where urban areas experience a higher temperature relative to their rural surroundings, especially at night (Oke 1987). There are two main approaches to quantify UHI including measurement of air temperature (T_{air}) in the canopy layer and land surface temperature (LST) (Schwarz et al. 2011, Sheng et al. 2017).

Due to the respective characteristics of these two types of temperature, the most common data sources used in studies on T_{air} and LST differ substantially (Oke et al. 2017,

Schwarz et al. 2012). For T_{air} collection, field measurements are generally used including fixed and mobile meteorological stations (Li et al. 2020, Unger et al. 2009). However, the limitation of number and uneven distribution of meteorological stations are serious shortcomings for T_{air} measurement in most urban areas, especially the lack of observations in densely built-up areas where the UHI effect is the strongest (Ho et al. 2016, Sheng et al. 2017); as for mobile measurement, in addition to the above problems, the accuracy of measurement is affected by the observation methodological design and route selection (Zhou et al. 2019). For LST data collection, the most common method is retrieving from satellite data (Tsou et al. 2017). Besides, infrared aircraft and camera are also used in some researches at local or street scale (Kelly et al. 1992, Unger et al. 2010). However, shortcomings still exist in these remote methods, such as limitation by weather conditions and observation frequency (Yang et al. 2020).

The interaction and correlation between urban T_{air} and LST have been proven in many studies (Roth et al. 1989, Schwarz et al. 2012), but it is worth noting that there are large differences between these two temperatures as a result of a high degree of spatial heterogeneity in thermal characteristics associated with urbanization (Prihodko and Goward 1997, Oke et al. 2017). In many studies on estimation of T_{air} based on remote sensing data, the T_{air} samples are scarce due to the lack of stations, and most of them are located in the suburbs far from the city centre, which cannot reflect the intra-urban air thermal environment exactly (Sheng et al. 2017, Pelta et al. 2016).

In our investigation, 24 meteorological stations, which were installed based on LCZs (Stewart and Oke 2012) and can represent all types of urban land covers in Szeged, were used to measure T_{air} (Unger et al. 2014). The objectives of our study are: (1) to analyse the connection between T_{air} and LST by using data from 2017 to 2019 and develop unary regression models for estimating T_{air} based on LST; (2) to validate the performance of the regression models by using data in 2016; (3) to add Normalised Difference Vegetation Index (NDVI) as the second independent variable to the regression models to develop binary regression models for T_{air} estimation and analyse the impact of NDVI on T_{air} ; (4) to analyse the influencing factors on the relationship between T_{air} and LST.

2. MATERIAL AND METHODS

2.1. Study area

We carried out our investigation in Szeged (46.3°N, 20.1°E), which is the largest city with a population of 162 000 in the southern region of the Great Hungarian Plain. The study area is a large flood plain and about 79 m above sea level. Tisza River passes through the city, but it is relatively narrow and its influence is negligible (Unger et al. 2001). This area is in Köppen's climatic region Cfa (Unger et al. 2020) with an annual mean temperature of 11.9°C, an amount of yearly precipitation of 508 mm, sunshine duration of 2049 hours and frequent drought (Harris et al. 2014). The study area covers a 10 km × 8 km rectangle in and around Szeged (Fig. 1).

2.2. Satellite data

In our study, LST were retrieved from Landsat-8 and MODIS. Our investigation focused on one season period from June to September during 4 years (2016–2019).

According to the weather condition, we selected 13 cloud free days to collect temperature data in Szeged region. Both Landsat-8 and MODIS are available in these 13 days. However, the data in some pixels of satellite images, especially at night, and some T_{air} obtained from meteorological stations are missing. After pairing LST with T_{air} , we got the final temperature data pairs (Table 1).

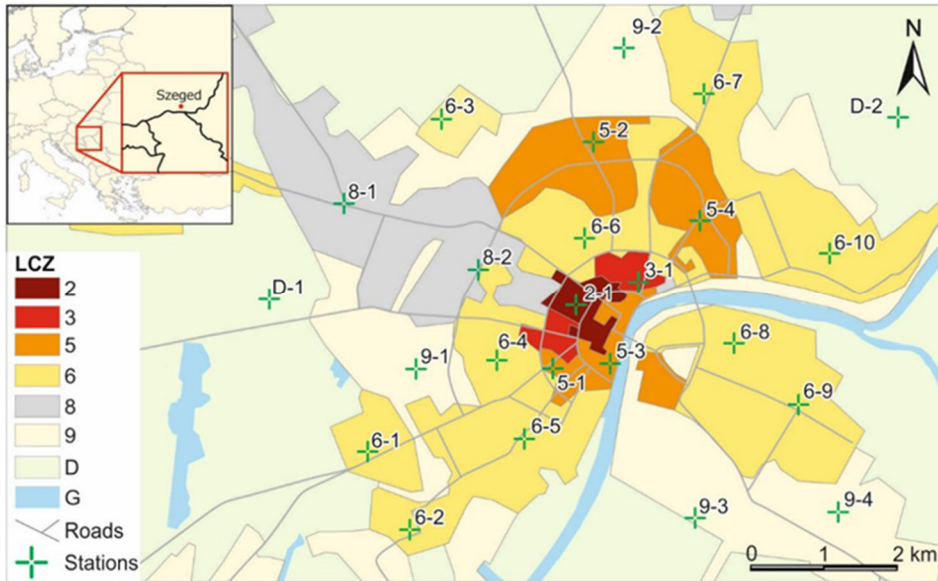


Fig. 1 Geographical location of Szeged and LCZs map of the study area with station sites of the urban meteorological network (marked by green crosses and digits referring to the zones) (Unger et al. 2018). For the explanation of LCZ classes see Stewart and Oke (2012).

Table 1 Information about the satellite data

Data source	Resolution	Observation time (UTC)	Amount of pairs of T_{air} and LST	
			2016	2017–2019
LST-Landsat-8	100 m	9:27	91	167
LST-MODIS-day	1000 m	10:54, 12:36	181	325
LST-MODIS-night	1000 m	1:30, 20:24	160	179
NDVI-Landsat-8	30 m	9:27	91	167

All processing and calculations of satellite data were carried out in Google Earth Engine (GEE) platform. GEE is a cloud computing platform designed to store and process huge data sets (at petabyte-scale) for analysis and ultimate decision making (Kumar and Mutanga 2018). Following the free availability of Landsat series in 2008, Google archived all the data sets and linked them to the cloud computing engine for open source use. The current archive of data includes those from other satellites, as well as Geographic Information Systems (GIS) based vector data sets, social, demographic, weather, digital elevation models, and climate data layers (Mutanga and Kumar 2019). The LST retrieval process was performed in the background on the Google cloud computing servers, with direct access to the GEE satellite data catalogue. Therefore, the application needs only a few seconds to produce Landsat-8 LST with no need for any computational resources from the user

(Parastatidis et al. 2017). In our investigation, the applications of GEE include LST retrieval from Landsat-8 and MODIS datasets, calculation of Normalized Difference Vegetation Index (NDVI) with Landsat-8 data and distance-weighted average calculation of LST and NDVI. All of the images were projected to UTM zone 34N and keep their original resolution.

(1) NDVI

NDVI image shows the vegetation extent of the area by analysing near-infrared and red spectral band data. NDVI is the index of photosynthetic activity in plant and it is the most commonly used vegetation spectral indices for crop growth monitoring (Pirotti et al. 2014). In this research, the purposes of calculating NDVI are: (1) to calculate the land surface emissivity (τ) for LST retrieval from Landsat-8 (Molnár 2016); (2) to create the binary regression model for T_{air} estimate. As the resolution of Landsat-8 (30 m) is higher than MODIS (250 m – 1 km), NDVI was calculated with Landsat-8 data according to the following equation (Tucker 1979):

$$NDVI = \frac{b5 - b4}{b5 + b4}$$

where b5 is the reflectance of near-infrared band and b4 is the reflectance of red band in Landsat-8 dataset.

(2) LST retrieval from satellite data

The Radiative Transfer Equation method was used to retrieve LST from Landsat-8 data. In this method, the main task is removing the atmospheric attenuation effects and calculation of land surface emissivity (Yu et al. 2014). The atmospheric profile was extracted from NASA's Atmospheric Correction Parameter Calculator (Barsi et al. 2003), which uses the National Centres for Environmental Prediction modeled atmospheric global profiles for a particular date, time and location as input. Then, the Moderate Resolution Atmospheric Transmission model was used to simulate atmospheric transmittance, upwelling and downwelling. The whole process can be expressed as the following equations:

$$L_{\lambda} = [\varepsilon B(T_s) + (1 - \varepsilon)L_{\downarrow}] \tau + L_{\uparrow}$$

$$B(T_s) = \frac{[L_{\lambda} - L_{\uparrow} - \tau(1 - \varepsilon)L_{\downarrow}]}{\tau \varepsilon}$$

where L_{λ} is the at-sensor radiance, L_{\uparrow} is the upwelling atmospheric radiance, L_{\downarrow} is the downwelling atmospheric radiance in $Wm^{-2}sr^{-1}\mu m^{-1}$, τ is the total atmospheric transmissivity between the surface and the sensor, and ε is the land surface emissivity, which can be calculated based on NDVI (Qin et al. 2004, Sobrino et al. 2004), $B(T_s)$ is the radiance of a blackbody target of kinetic temperature T_s in $Wm^{-2}sr^{-1}\mu m^{-1}$. Then an inversion of Planck's Law was applied to derive the kinetic skin temperature using the following equation:

$$T_s = \frac{K_2}{\ln \frac{K_1}{B(T_s) + 1}}$$

where K_1 and K_2 are the thermal band calibration constants found in the Landsat-8 metadata files ($K_1=774.89$, $K_2=1321.08$).

As for MODIS data, the daily LST and Emissivity products were used over Szeged. The version-5 products from 2016 to 2019 were collected for this study, which are abbreviated as MOD11A1 and MYD11A1 and have a spatial resolution of approximately 1 km (Sun et al. 2015, Wan 2008). MODIS data were collected by both the Terra and Aqua Sun-synchronous satellites. Terra passes the equator from north to south (descending node) at approximately 10:30 a.m. and Aqua passes the equator from south to north (ascending node) at approximately 1:30 p.m. local time. The land-surface thermal radiation can be obtained at least four times each day in our study area. Nevertheless, there are some areas without LST data in MODIS images, especially at night, so the final daytime data is twice the night-time data. The details of NDVI and both LSTs from Landsat-8 and MODIS are shown in Table 1.

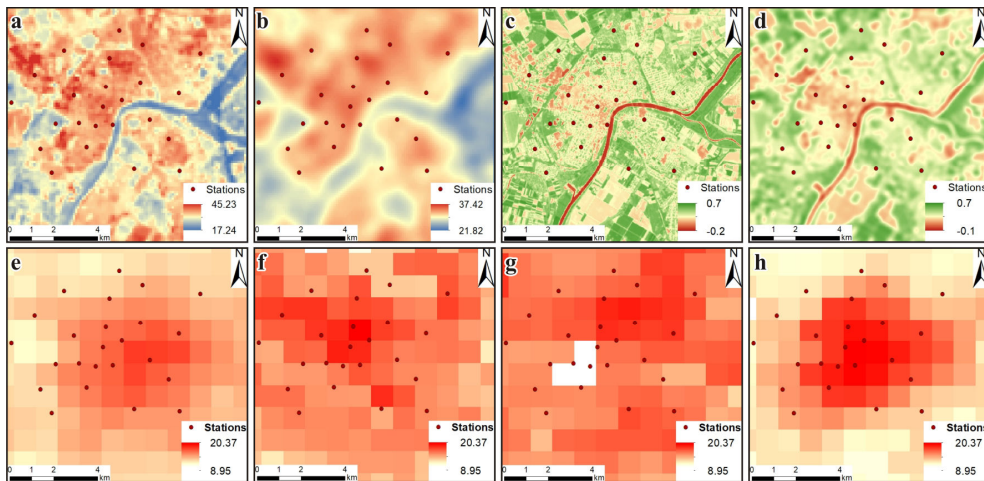


Fig. 2 Examples of spatial patterns of LST and NDVI: (a) and (c) LST and NDVI from Landsat-8, 2017-06-24, 9:27 (UTC), respectively; (e–h) LST from MODIS MOD11A1 and MYD11A1, 2016-07-07, 1:30, 10:54, 12:36 and 20:24 (UTC), respectively; (b) and (d) distance-weighted average of LST and NDVI, respectively

(3) Distance-weighted average

MODIS and Landsat-8 images have different spatial resolutions. Therefore, to be comparable and usable in statistical analysis, the distance-weighted spatial average of NDVI and $LST_{Landsat-8}$ was calculated. As shown in Figs. 2b and d, the value in each pixel is the distance-weighted average of all pixel in a 1 km square centered this pixel (Unger et al. 2009). Considering that the T_{air} is affected by LST and air turbulence and these influence factors on T_{air} at 4 m height may extend over a local scale, hence it is reasonable to choose the range of 1 km to calculate the spatial average LST. This calculation process was carried out in GEE. As for the MODIS data, we used the original value (Fig. 2).

2.3. T_{air} data collection

T_{air} data were obtained from a meteorological monitoring network in Szeged. This monitoring network was established in Szeged within the framework of an EU project (URBAN-PATH 2016, urban-path.hu). 24 stations were installed to measure T_{air} and relative humidity every 10 minutes. The locations of the stations were selected based on the distribution of LCZs in Szeged (Lelovics et al. 2014, Unger et al. 2018). All of stations have to be representative of the LCZs within the city and spatial pattern of the network has to be capable of revealing the spatial structure of the UHI (Unger et al. 2015). The accuracy of the thermal sensors is 0.4°C. The consoles are mounted on lamp posts at the height of 4 m above the ground for security reasons. As the air in the urban canyon is well-mixed, the temperature measured at this height is representative of the lower air layers (Nakamura and Oke 1988, Unger et al. 2014). When we paired T_{air} with LST, if their observation time was not exactly synchronous, we chose the closest T_{air} to the LST with the temporal interval of less than five minutes (Gál et al. 2016).

2.4. Methods of statistical analysis

Statistical analysis was performed by SPSS 25.0 and Microsoft Excel 2019. Correlation, error and regression analysis were employed in this study. Pearson correlation coefficient (r) was computed to evaluate the correlation between LST and T_{air} . Root-mean-square error (RMSE) and mean-absolute error (MAE) were computed to quantitatively evaluate the difference between LST and T_{air} . Then, linear regression models were created to estimate T_{air} based on LST and NDVI during 2017–2019. Finally, the T_{air} , LST and NDVI data in 2016 were used to validate the performance of these models. For this validation, the RMSE and MAE between estimated T_{air} and measured T_{air} were calculated and compared (Janssen and Heuberger 1995, Hrisko et al. 2020). The unary and binary regression models are shown as the following equations:

$$T_{\text{air}}=a \cdot \text{LST}+e$$

$$T_{\text{air}}=a \cdot \text{LST}+b \cdot \text{NDVI}+e$$

3. RESULTS

3.1. Connection and error analysis between T_{air} and LST

Relationships between T_{air} and LST over 9-day periods from 2017 to 2019 were calculated using 671 data pairs (Fig. 3). As error analyse (RMSE and MAE) shows (Fig. 3 a–c), errors between T_{air} and $\text{LST}_{\text{Landsat-8}}$ were largest with an RMSE of 6.1°C and an MAE of 5.6°C, and the errors between T_{air} and $\text{LST}_{\text{MODIS-Day}}$ were relatively smaller with an RMSE of 4.2°C and an MAE of 3.6°C, the smallest errors (RMSE=2.3°C and MAE=2.0°C) appear at night when $\text{LST}_{\text{MODIS-Night}}$ were used to compare with T_{air} . In Pearson’s correlation analysis, the stronger connection between T_{air} and LST appears at night ($\text{LST}_{\text{MODIS-Night}}$, $r=0.97$, $P<0.01$) compared with $\text{LST}_{\text{Landsat-8}}$ ($r=0.89$, $P<0.01$) and $\text{LST}_{\text{MODIS-Day}}$ ($r=0.89$, $P<0.01$). In general, the difference between T_{air} and LST varies from day to night; T_{air} has a stronger connection and smaller errors with LST at night. When the influence of solar radiation ceases, the energy exchange between air and surface tends to be stable at night; the difference

between T_{air} and LST decreases and the correlation increases significantly, which is the same as the results of previous studies (e.g. Sun et al. 2015). $LST_{MODIS-Day}$ has the same connection but smaller errors with T_{air} compared with $LST_{Landsat-8}$, which may be caused by the inherent differences between these two data sources and their different observation time.

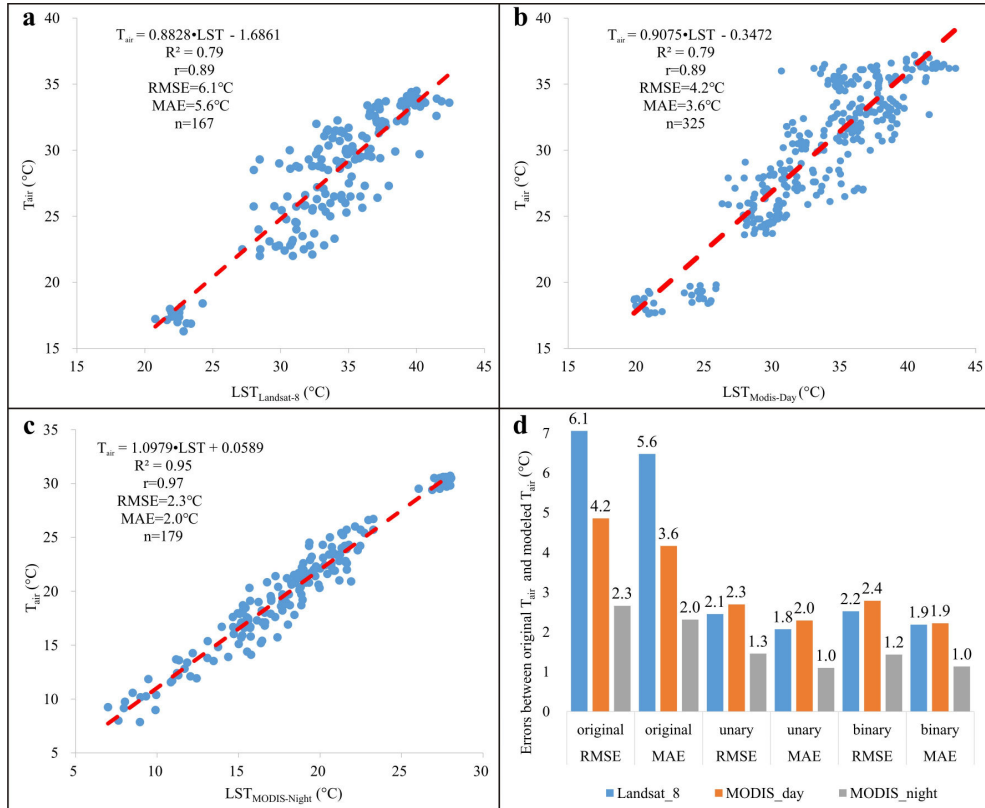


Fig. 3 (a), (b) and (c): Results of regression, correlation and error analysis between T_{air} and $LST_{Landsat-8}$, $LST_{MODIS-Day}$ and $LST_{MODIS-Night}$, respectively, from 2017 to 2019; (d): The error analysis between observed T_{air} and estimated T_{air} in 2016

3.2. Development and validation of regression models

The differences between T_{air} and LST are obvious and unignored, despite their moderate to high correlation. So we trained regression models based on T_{air} and LST data during 2017–2019 to estimate T_{air} (Fig. 3a–c). The results showed that the value of R^2 was 0.79 ($P < 0.01$) when $LST_{Landsat-8}$ and $LST_{MODIS-Day}$ were used in models, which means 79% of the variation of T_{air} can be explained by the LST. In addition, the night-time model, with a higher R^2 of 0.97 ($P < 0.01$), can perform better than that during daytime, which means almost all of the variation of T_{air} can be explained by the LST. Then, these regression equations were validated by using the LST data in 2016. We estimated T_{air} basing on $LST_{Landsat-8}$ and LST_{MODIS} in 2016 and calculated the RMSE and MAE between real T_{air} and estimated T_{air} (Fig. 3d). The results indicated that all models could reduce the error to less than 2.5°C,

especially when $LST_{MODIS-Night}$ were used in the model with an RMSE of $1.3^{\circ}C$ and MAE of $1.0^{\circ}C$, which means that T_{air} can be accurately estimated using only LST at night.

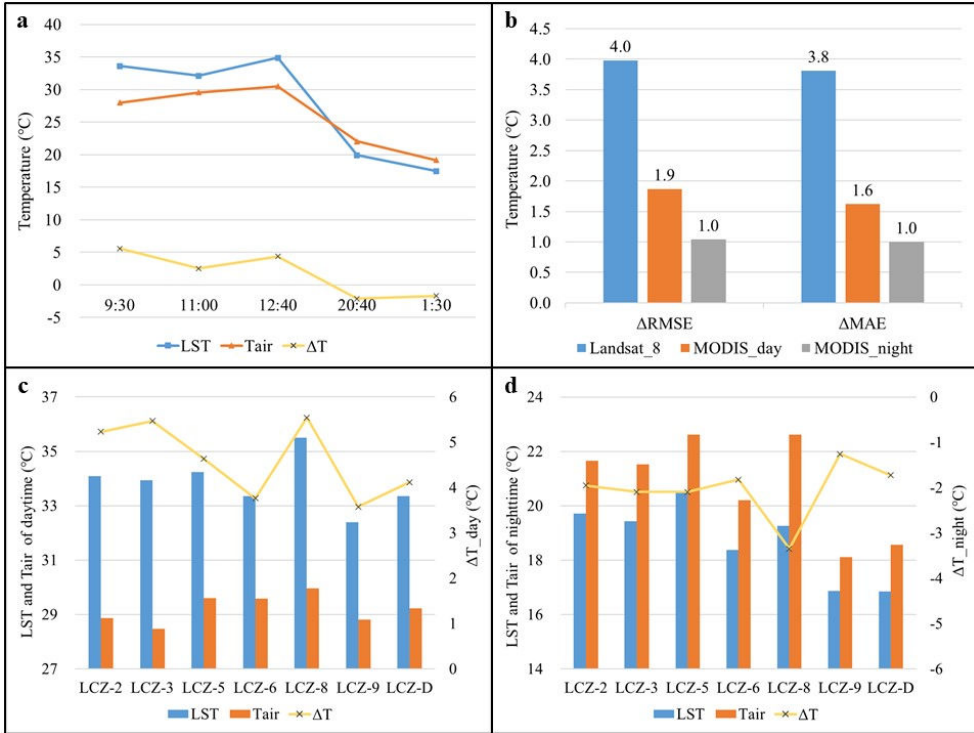


Fig. 4 (a) Average of LST, T_{air} and the difference between LST and T_{air} (ΔT) at 5 observation time (9:30, 11:00, 12:40, 20:40 and 1:30); (b) The difference between original errors and estimated errors; (c) and (d): Mean value of T_{air} , LST and temperature difference (ΔT) between T_{air} and LST by LCZs during daytime and nighttime, respectively

In consideration of the effect of vegetation on the urban thermal environment (Shiflett et al. 2017), we tried to add NDVI into the regression models to develop binary regression models. The coefficients of determination (R^2) of models based on $LST_{Landsat-8}$, $LST_{MODIS-Day}$ and $LST_{MODIS-Night}$ were 0.80, 0.80 and 0.95 ($P < 0.01$), respectively, which means that these models can effectively estimate T_{air} . In order to compare with unary regression models, we calculated the RMSE and MAE between observed T_{air} and estimated T_{air} based on both models without and with NDVI (Fig. 3d). Unexpectedly, we saw a slight increase in errors when binary regression models were used, only $RMSE_{MODIS-Night}$ and $MAE_{MODIS-Day}$ decreased from $1.3^{\circ}C$ to $1.2^{\circ}C$ and from $2.0^{\circ}C$ to $1.9^{\circ}C$, respectively. This results indicate that the role of urban vegetation may not be important for estimating T_{air} .

4. DISCUSSION

4.1 Comparison of Landsat-8 and MODIS

The results of Section 3.1 showed that T_{air} had the same connection with $LST_{\text{Landsat-8}}$ as with $LST_{\text{MODIS-Day}}$. However, it should be noted that errors between T_{air} and $LST_{\text{Landsat-8}}$ are obviously higher than errors between T_{air} and LST_{MODIS} , which is mainly the result of high $LST_{\text{Landsat-8}}$. We calculated the average of LST, T_{air} and the difference between LST and T_{air} (ΔT) at 5 observation time (9:30, 11:00, 12:40, 20:40 and 1:30, Fig. 4a). When Landsat-8 was used to retrieve LST (9:30), the average $LST_{\text{Landsat-8}}$ was relatively higher than the average LST_{MODIS} at 11:00, which was inconsistent with the fluctuation of T_{air} . This differential can be explained by the inherent error between Landsat-8 data and MODIS data, which caused the highest ΔT , RMSE and MAE at 9:30.

We also compared the performance of regression models based on $LST_{\text{Landsat-8}}$, $LST_{\text{MODIS-Day}}$ and $LST_{\text{MODIS-Night}}$ by calculating ΔRMSE and ΔMAE (Fig. 4b). We found that the model based on $LST_{\text{Landsat-8}}$ could reduce the errors by nearly 4°C, which was the largest among these three values presented. Furthermore, the errors based on $LST_{\text{Landsat-8}}$ were smaller than that based on $LST_{\text{MODIS-Day}}$ after regression calculating (Fig. 3d), indicating that Landsat-8 data can perform better than MODIS-Day data in T_{air} estimation. On the one hand, the larger difference between $LST_{\text{Landsat-8}}$ and T_{air} caused the possibility of larger ΔRMSE and ΔMAE ; on the other hand, the climatological stations were not accurately located in the center of each pixel as a result of the wide pixel range of MODIS images, which caused a spatial error between T_{air} and LST_{MODIS} . This spatial error likely caused the differential of performance of estimation models based on MODIS-Day and Landsat-8 data.

4.2 Spatio-temporal variability of T_{air} and LST

As mentioned in Section 2, all 24 climatological stations are located in specific LCZs which are distinguished based on the characteristics of land surface (Lelovics et al. 2014, Unger et al. 2018). We calculated the mean value of T_{air} , LST and temperature difference (ΔT) between T_{air} and LST in each specific LCZ. As shown in Fig. 4c and 4d, the difference of LSTs among these LCZs were distinct, which indicated that the spatial variability of LST was greater than T_{air} during daytime. According to Oke et al. (2017), the variability in geometric, radiative, thermal, moisture and aerodynamic properties of urban surface underlie the greater spatial variability of LST compared to T_{air} , particularly during daytime. At that time, the most dominant surfaces with relatively high LST are roads, residential and industrial areas, etc. which are covered by artificial pavements, such as LCZs 2, 3 and 8. These areas are characterized by higher thermal conductivity and heat capacity, and in addition, there is less evaporative cooling effect over these surfaces. The influencing factors on T_{air} are different from the ones on LST. T_{air} is mainly affected by radiation, conduction and convection. During daytime, T_{air} is characterized by relatively high homogeneity as a result of country breeze and local airflow (Beranová and Huth 2005), which usually causes UHI to decline or even disappear. At night, T_{air} has a similar spatial variability to LST when country breeze and local airflow weaken and longwave radiation of surface dominates. Because of the spatial variability of T_{air} and LST, the spatial variability of ΔT is also obvious.

5. CONCLUSIONS

This study utilized Landsat-8 data and MODIS data to retrieve urban land surface temperature (LST) and measured urban air temperature (T_{air}) by 24 climatological stations in the period of 2016–2019 in Szeged. We compared LST and T_{air} by using error and connection analysis, then we developed and validated regression equations for estimating T_{air} based on LST, NDVI and T_{air} . Finally, by calculating the mean of LST, T_{air} and their difference at specific observation time and LCZ, we analysed the influencing factors on the relationship between T_{air} and LST. Based on our research results, we conclude:

(1) T_{air} and LST have a strong enough correlation during both day and night. The correlation at night is stronger ($r=0.97$) with lower errors (RMSE=2.3°C and MAE=2.0°C) and better regression model performance ($R^2=0.95$, $P<0.01$);

(2) All regression models can effectively estimate T_{air} , especially at night. The errors can be reduced below 2.5°C during the day and below 1.5°C at night. NDVI cannot enhance the performance of the T_{air} prediction models. On the contrary, a slight weakening can be observed when NDVI was added in models;

(3) The difference between $LST_{\text{Landsat-8}}$ and LST_{MODIS} is obvious in T_{air} estimation, which indicated that we should consider this difference when combining different satellite data. The difference in the temporal and spatial resolution of satellite imagery, as well as certain weather conditions, are limitations on the use of remote sensing data;

(4) The relationship between LST and T_{air} has obvious spatial and temporal variability. LST is higher than T_{air} during daytime, and the opposite is true at night. The difference between T_{air} and LST is relatively high in LCZs 2, 3 and 8 with more artificial surfaces.

Overall, in our study, 24 climatological stations distributed in 7 LCZs were used in and around urban area of Szeged, which is our advantage in T_{air} estimate compared with other studies. The models developed for estimating T_{air} make it possible to use LST as a substitute for T_{air} measurement in cities without enough climatological station.

Acknowledgement: This paper was supported by Stipendium Hungaricum Programme founding by the Hungarian Government.

REFERENCES

- Barsi JA, Barker JL, Schott JR (2003) An atmospheric correction parameter calculator for a single thermal band earth-sensing instrument. 2003 IEEE International Geoscience and Remote Sensing Symposium, Toulouse, France. 3014-3016
- Beranová R, Huth R (2005) Long-term changes in the heat island of Prague under different synoptic conditions. *Theor Appl Climatol* 82:113-118
- Gál T, Skarbit N, Unger J (2016) Urban heat island patterns and their dynamics based on an urban climate measurement network. *Hung Geogr Bull* 65:105-116
- Harris I, Jones PD, Osborn TJ, Lister DH (2014) Updated high-resolution grids of monthly climatic observations – the CRU TS3.10 Dataset. *Int J Climatol* 34:623-642
- Ho H, Knudby A, Xu Y, Hodul M, Aminipouri M (2016) A comparison of urban heat islands mapped using skin temperature, air temperature, and apparent temperature (Humidex), for the greater Vancouver area. *Sci Total Environ* 544: 929-938
- Hrisko J, Ramamurthy P, Yu Y, Yu P, Vázquez D (2020) Urban air temperature model using GOES-16 LST and a diurnal regressive neural network algorithm. *Rem Sens Environ* 237:111495
- Janssen PH, Heuberger PS (1995) Calibration of process-oriented models. *Ecol Model* 83:55-66

Model development for the estimation of urban air temperature based on surface temperature and NDVI – a case study in Szeged

- Kelly RB, Smith EA, MacPherson JI (1992) A comparison of surface sensible and latent heat fluxes from aircraft and surface measurements in FIFE 1987. *J Geophys Res* 97:18445-18453
- Kalnay E, Cai M (2003) Impact of urbanization and land-use change on climate. *Nature* 423:528-531
- Kumar L, Mutanga O (2018) Google Earth Engine applications since inception: usage, trends, and potential. *Rem Sens-Basel* 10:1509
- Lelovics E, Unger J, Gál T, Gál CV (2014) Design of an urban monitoring network based on Local Climate Zone mapping and temperature pattern modelling. *Clim Res* 60:51-62
- Li H, Meng H, He R, Lei Y, Guo Y, Ernest A, Jombach S, Tian G (2020) Analysis of cooling and humidification effects of different coverage types in Small Green Spaces (SGS) in the context of urban homogenization: A case of HAU Campus green spaces in summer in Zhengzhou, China. *Atmosphere* 11:862
- Molnár G (2016) Analysis of land surface temperature and NDVI distribution for Budapest using Landsat 7 ETM+ data. *Acta Climatol* 49-50:49-61
- Mutanga O, Kumar L (2019) Google Earth Engine applications. *Rem Sens-Basel* 11:591
- Nakamura Y, Oke TR (1988) Wind, temperature and stability conditions in an east–west oriented urban canyon. *Atmos Environ* 22: 2691-2700
- Oke TR (1987) *Boundary Layer Climates*. Methuen, London
- Oke TR, Mills G, Voogt JA (2017) *Urban Climates*. University Press, Cambridge
- Parastatidis D, Mitraka Z, Chrysoulakis N, Abrams M (2017) Online global land surface temperature estimation from Landsat. *Rem Sens-Basel* 9:1208
- Pelta R, Chudnovsky A, Schwartz J (2016) Spatio-temporal behavior of brightness temperature in Tel-Aviv and its application to air temperature monitoring. *Environ Poll* 208:153-160
- Peng J, Xie P, Liu Y, Ma J (2016) Urban thermal environment dynamics and associated landscape pattern factors: A case study in the Beijing metropolitan region. *Rem Sens Environ* 173:145-155
- Pirotti F, Parraga MA, Stuardo E, Dubbini M, Masiero A, Ramanzin M (2014) NDVI from Landsat 8 vegetation indices to study movement dynamics of Capra ibex in mountain areas. In: ISPRS Technical Commission VII Symposium, XL-7:147-153
- Prihodko L, Goward S (1997) Estimation of air temperature sensed surface observations. *Rem Sens Environ* 60:335-346
- Qin Z, Li W, Xu B, Zhang W (2004) Estimation method of land surface emissivity for deriving land surface temperature from Landsat TM6 data. *Adv Marine Sci* 22:129-137
- Roth M, Oke TR, Emery WJ (1989) Satellite-derived urban heat islands from three coastal cities and the utilization of such data in urban climatology. *Int J Rem Sens* 10:1699-1720
- Schwarz N, Schlink U, Franck U, Großmann K (2012) Relationship of land surface and air temperatures and its implications for quantifying urban heat island indicators – An application for the city of Leipzig (Germany). *Ecol Indic* 18:693-704
- Sheng L, Tang X, You H, Gu Q, Hu H (2017) Comparison of the urban heat island intensity quantified by using air temperature and Landsat land surface temperature in Hangzhou, China. *Ecol Indic* 72:738-746
- Shiflett S, Liang L, Crum S, Feyisa G, Wang J, Jenerette G (2017) Variation in the urban vegetation, surface temperature, air temperature nexus. *Sci Total Environ* 579:495-505
- Sobrino JA, Jiménez-Muñoz JC, Paolini L (2004). Land surface temperature retrieval from LANDSAT TM 5. *Rem Sens Environ* 90: 434-440
- Stewart ID, Oke TR (2012) Local Climate Zones for urban temperature studies. *Bull Am Meteorol Soc* 93:1879-1900
- Sun H, Chen Y, Zhan W (2015) Comparing surface- and canopy-layer urban heat islands over Beijing using MODIS data. *Int J Rem Sens* 36: 5448-5465
- Tsou J, Zhuang J, Li Y, Zhang Y (2017) Urban heat island assessment using the Landsat 8 data: A case study in Shenzhen and Hong Kong. *Urban Sci* 1:10-31
- Tucker C J (1979) Red and photographic infrared linear combinations for monitoring vegetation. *Rem Sens Environ* 8:127-150
- Unger J, Sümeghy Z, Gulyás Á, Bottyán Z, Mucsi L (2001) Land-use and meteorological aspects of the urban heat island. *Meteorol Appl* 8:189-194
- Unger J, Gál T, Rakonczai J, Mucsi L, Szatmári J, Tobak Z, Leeuwen B, Fiala K (2009). Air temperature versus surface temperature in urban environment. In: *The 7th International Conference on Urban Climate*, Yokohama, Japan
- Unger J, Gál T, Rakonczai J, Mucsi L, Szatmári J, Tobak Z, Leeuwen B, Fiala K (2010) Modeling of the urban heat island pattern based on the relationship between surface and air temperatures. *Időjárás* 114:287-302

- Unger J, Savic SM, Gál T, Milosevic DD (2014) Urban climate and monitoring network system in European cities. University of Novi Sad, University of Szeged, Novi-Sad, Szeged
- Unger J, Gál T, Csépe Z, Lelovics E, Gulyás Á (2015) Development, data processing and preliminary results of an urban human comfort monitoring and information system. *Időjárás* 119:337-354
- Unger J, Skarbit N, Gál T (2018) Absolute moisture content in mid-latitude urban canopy layer, part 2: results from Szeged, Hungary. *Acta Climatol* 51-52:47-56
- Unger J, Skarbit N, Kovács A, Gál T (2020) Comparison of regional and urban outdoor thermal stress conditions in heatwave and normal summer periods: A case study. *Urban Clim* 32:100619
- Wan Z (2008) New refinements and validation of the MODIS land-surface temperature/emissivity products. *Rem Sens Environ* 112:59-74
- Yang C, Yan F, Zhang S (2020) Comparison of land surface and air temperatures for quantifying summer and winter urban heat island in a snow climate city. *J Environ Manage* 265:110563
- Yu X, Guo X, Wu Z (2014) Land surface temperature retrieval from Landsat 8 TIRS – Comparison between Radiative Transfer Equation-Based Method, Split Window Algorithm and Single Channel Method. *Rem Sens-Basel* 6:9829-9852
- Zhou B, Kaplan S, Peeters A, Kloog I, Erell E (2019) “Surface,” “satellite” or “simulation”: Mapping intra-urban microclimate variability in a desert city. *Int J Climatol* 40:3099-3117

URBAN HEAT ISLAND STUDIES IN SZEGED, HUNGARY – AN OVERVIEW BASED ON PAPERS PUBLISHED OVER THE PAST FORTY YEARS (1980–2020)

J UNGER

*Department of Climatology and Landscape Ecology, University of Szeged, Egyetem u. 2., 6720 Szeged, Hungary
E-mail: unger@geo.u-szeged.hu*

Summary: The overview summarizes briefly the contents and results of the papers published in journals dealing with urban heat island investigations in Szeged, Hungary between 1980 and 2020. The thermal data they used came from urban station networks, mobile measurements, local-scale simulations as well as aerial and satellite images.

Keywords: urban heat island, Szeged, Hungary

1. INTRODUCTION

This paper lists in chronological order the papers published in journals (in Hungarian and in English) related to the urban heat island (UHI) investigations in Szeged (Hungary) over the last forty years. It summarizes the contents and results of the papers briefly, partly based on their edited, abbreviated abstracts when available. The overview focuses on the period of 1980–2020 taking into account the first published article on the subject (Károssy and Gyarmati 1980).

The studies listed relied essentially on four thermal data sources in Szeged, namely: (i) manually observed data of the first urban network (11 stations) working between 1977 and 1981; (ii) city-wide mobile measurements between 1999 and 2003, as well as in 2008; (iii) automatically observed and stored data of the second urban network (24 stations) working from 2014; (iv) data of local-scale simulations from 2016. There are a few studies which analysed in part other data sources (e.g. aerial and satellite images). From 2013 most studies used the Local Climate Zone (LCZ) system to characterize the different land use/land cover types in and around the urban area.

Szeged is a medium-sized city with a population of around 160 thousands. It is located in the south-eastern part of Hungary (46.3°N, 20.1°E) at 79 m above sea level on a flat flood plain. The River Tisza passes through the city, otherwise, there are no large water bodies nearby. The river is relatively narrow and according to our earlier investigation its influence is negligible (Unger et al. 2000, 2001e). These environmental conditions make Szeged a suitable place for studying of an almost undisturbed urban climate.

Most of the territory of Hungary belongs to Köppen's climatic region Cf (temperate warm climate with a fairly uniform annual distribution of precipitation). Climatic subregions are distinguished using the mean temperature of vegetative season (t_{VS} in °C) and aridity index ($H = Q^*/(L_V \cdot P)$ where Q^* is the annual mean net radiation in MJm^{-2} , L_V is the latent heat of evaporation in MJkg^{-1} and P is the annual mean precipitation in kgm^{-2}). Szeged is in

the „warm-dry” subregion by this classification which is characterized by $t_{VS} > 17.5^{\circ}\text{C}$ and $H > 1.15$ (slightly arid). Two half years can be distinguished as the heating (from October until April) and the non-heating (from April until October) seasons. Szeged has an administration area of 281 km² but the urbanized area covered only about 40 km². The base of its street network is a circuit-avenue system. Different land-use types are present including a densely-built centre with medium-wide streets (LCZs 2 and 3) and large housing estates of high concrete buildings set in wide green spaces (LCZ 5). There are zones used for industry and warehousing (LCZ 8), areas occupied by detached houses (LCZs 6 and 9), considerable open spaces along the riverbanks, in parks, and around the city’s outskirts (LCZs D and C) (Unger et al. 2004, 2015).

2. CHRONOLOGICAL LISTING

2.1. Studies based on the data of the first urban station network

Development of urban heat island in the air of Szeged (Károssy, Gyarmati 1980):

This paper used the data series of the 11-station network in Szeged. The temperature values were read manually at 4 times per day. The minimum and maximum temperature values of the cloudless and calm days between 1977 and 1979 were examined. There were 123 days in this period which were all connected with anticyclonic weather types. The authors averaged the temperature values by seasons and drew the isolines of urban-rural differences for both extreme temperatures. The isolines of mean differences took form most typically in winter in both cases (the differences in minimum temperature exceed 3°C in the city centre).

Urban climate measurements in Szeged (Pelle 1983):

This study dealt with the effects of a strong cold front of 19th February 1978 for a few days on the urban-rural differences of minimum temperature based on the data series of the above mentioned station network in Szeged. The isotherms of the differences were drawn for each day. On the first day the differences were normally, but on the 20th they suddenly increased (the excess of the centre was over 8°C), then they gradually decreased on the 21st and 22nd. So it could be seen that very remarkable temperature differences can develop in certain macrosynoptical situations between the city and its rural surroundings.

The seasonal system of urban temperature surplus in Szeged, Hungary (Unger 1992a):

This study investigated the magnitude and pattern of the urban temperature surplus based on the station network of Szeged between 1977 and 1980 and focused on the sunny, advection-free days. By the help of the seasonal means calculated from the daily mean temperatures of such days, the seasonal patterns of the temperature excess were presented. Accordingly, the city centre was averagely 1.5–2.1°C warmer than the surroundings, but the urban-rural temperature difference exceed even 2.5°C.

Diurnal and annual variation of the urban temperature surplus in Szeged, Hungary (Unger 1992b):

This paper examined the relationship between the urban morphological types of Szeged and the urban heat excess from 1978 to 1980. The monthly mean temperature differences of several stations representing different built-up areas reflected the built-up densities differently by months and by observation times. The temperature increasing effect of the city appeared in the centre most obviously and the largest differences occurred at 1h at night in early autumn (over 4°C). The row of built-up types as a function of decreasing heat excess were as follow: housing estate with tall concrete buildings, loosely built inner area, area between outskirts and housing estate with tall concrete buildings and outskirts.

Some features of urban influence on temperature extremities (Unger, Ondok 1995):

This paper dealt with the influence of different built-up areas on the spatial distribution of numbers of summer, winter and frost days, as well as of dates of the last and first frost days and the length of the frost-free period based on the data series of the urban network in Szeged. The results revealed that the distribution patterns largely depended on the density and building materials of the built-up areas.

Heat island intensity with different meteorological conditions in a medium-sized town: Szeged, Hungary (Unger 1996a):

In this study the thermal effects of Szeged was investigated based on minimum temperatures of urban and rural stations between 1978 and 1980. The UHI effect was examined by revelation of the relationships between UHI intensity and macrosynoptic types, cloudiness, wind speed as well as the combination of cloud amount and wind speed. Anticyclonic weather situations, little or no cloud coverage, and calm or slight wind were favourable for a strong development of the heat island effect. In the case of extreme UHIs the domination of anticyclonic weather types was almost absolute.

Relationship between urban heat island and wind on the example of Szeged (Unger 1996b):

In this study the relationships between UHI intensity and wind speed/directions were investigated based on measurements of urban and rural stations between 1978 and 1980 in Szeged. As the results showed the relationship between wind speed and UHI was reversed, the stronger the wind, the weaker the intensity. Additionally, the UHI was stronger in the case of western wind, which could be explained by the fact that the rural station was located west of the city.

Urban-rural difference in the heating demand as a consequence of the heat island (Unger, Makra 2007); The effect of urban heat island on heating energy demand in Szeged (Unger 1997):

The database of these studies was provided by an urban-rural meteorological station-pair in the period of 1978–1980 in Szeged. The climatic characteristics of the region in the mentioned three years and in the period of 1961–1990 did not show significant differences, which was certified by the application of a special case of the Student t-test. Therefore, the

results, related to the climate-modifying effect of the city, could be extended to a longer period as well. According to the results, the development of the UHI reduced the number of heating days (HD) and heating degree-days (HDD) thus it reduced the duration of the heating season and the quantity of energy consumption in the city. Monthly means of the urban and rural HDs and HDDs showed that the heating season was shorter by more than 3 weeks and the energy demand was about 10% lower in the city than in the rural areas.

2.2. Studies based on mobil measurement data

*A model for the maximum urban heat island in Szeged, Hungary (Unger et al. 1999a);
The spatial extent of the maximally developed urban heat island in spring in Szeged
(Unger et al. 1999b):*

In these studies the efforts concentrated on the investigation of maximum development of the UHI in Szeged based on mobile measurements in the spring of 1999. Tasks included the determination of spatial distribution of mean maximum UHI intensity and modelling the existing conditions in the measurement period. Statistical methods were used to examine the effects of invariable parameters (land-use characteristics, distance from the city centre determined in a grid network) and by variable parameters (wind speed, temperature) on thermal conditions. The results indicated isotherms increasing in rather regular concentric shapes from the suburbs toward the inner urban areas. Strong relationship existed between urban thermal excess and land-use features. In addition, meteorological conditions determined to a great extent the UHI intensity at the time of its maximum development.

Land-use and meteorological aspects of the urban heat island (Unger et al. 2001b):

This study examined the influence of urban and meteorological factors on the near-surface air temperature field of Szeged, using mobile and stationary measurements under different weather conditions between March and August 1999. Tasks included the determination of the spatial distribution of seasonal mean maximum UHI intensity and modelling of existing conditions. Multiple correlation and regression analyses were used to examine the effects of urban parameters (land-use characteristics and distance from the city centre determined in a grid network) and of meteorological parameters (wind speed, temperature) on thermal conditions in the study area. The results indicated isotherms increasing in regular concentric shapes from the suburbs towards the inner urban areas where the mean maximum UHI intensity reaches more than 3°C in the studied periods. Strong relationship existed between urban thermal excess and distance, as well as built-up ratio. In contrast, meteorological conditions did not have any significant effect on the UHI intensity at the time of its maximum development.

*Urban heat island development affected by urban surface factors (Unger et al. 2000);
Urban temperature excess as a function of urban parameters in Szeged, Part 1:
Seasonal patterns (Unger et al. 2001c); Urban temperature excess as a function of
urban parameters in Szeged, Part 2: Statistical model equations (Unger et al. 2001a):*

These studies examined the spatial and quantitative influence of urban factors on the air temperature pattern of Szeged using mobile measurements under different weather

conditions between March 1999 and February 2000. Their efforts concentrated on the UHI in its peak development during the diurnal cycle. Tasks included the determination of spatial distribution of mean daily maximum UHI intensity, using of standard kriging procedure and the determination of statistical model equations in the one-year study period, as well as in the heating and non-heating seasons. Multiple correlation and regression analyses were used to reveal the effects of urban surface parameters (land-use characteristics and distance from the city centre determined in a grid network) on the UHI patterns. The results indicated isotherms increasing in regular concentric shapes from the suburbs toward the inner urban areas with a seasonal variation in the UHI magnitude. As the patterns showed, strong relationship existed between urban thermal excess and built-up density. In the city centre, the mean UHI intensity reached more than 2.6°C (year), 3.1°C (non-heating) and 2.1°C (heating). According to the model equations, strong relationships existed between urban thermal excess and distance, as well as built-up ratio, but the role of water surface was negligible.

Temperature cross-section features in an urban area (Unger et al. 2001e); Urban temperature surplus: cross-sectional studies in Szeged (Unger, Sümeghy 2001):

These studies examined the connection between the built-up urban surface and air temperature in Szeged. Data were collected by mobile measurements under different weather conditions between March 1999 and February 2000. The efforts concentrated on investigating the maximum diurnal development of the UHI along an urban cross-section. According to the results, the UHI intensity changed according to seasons, as a consequence of the prevailing weather conditions. The role of cloudiness and wind speed on the temporal variation of the largest UHI was clearly recognized during most of the time in the studied period. The seasonal profiles followed remarkably well the general cross-section of the typical UHI described by Oke (1987) who defined its characteristic parts as 'cliff', 'plateau' and 'peak'. The usefulness of the normalized values in the investigation was proved, as the form of the seasonal mean UHI profile was independent of the seasonal climatological conditions, and was determined to a high degree by urban surface factors. As a conclusion, a modified model describing the metropolitan temperature variable for cities situated in simple geographical conditions was suggested: it was equal to the sum of components of the basic climate of the region and of the production of urbanization in surface, where this last term was a multiplication of weather and urban surface factors.

Seasonal case studies on the urban temperature cross-section (Sümeghy, Unger 2003a); Temperature modification effect of settlements – Heat island investigations in Szeged (Sümeghy, Unger 2003b):

In these papers the investigations concentrated on the spatial distribution and temporal dynamics of the nocturnal UHI, using mobile measurements under different weather conditions in the periods of March 1999–February 2000 and April 2002 – March 2003 in Szeged. Task also included the revelation of building-up and building-down of the UHI along an urban cross-section studying example cases by seasons and the explanation of their features using land-use and meteorological parameters. The UHI profiles were rather perfect with the highest values in the city centre and a few hours after sunset. However, some asymmetry occurred in the isotherms because they were always shifted a bit to the eastern edge of the transect. It could be attributed to the influence of the highest built-up density of this neighbourhood. For example, in the case of the summer night using normalized UHI values

some interesting features in the profiles emerged. Presumably, the changes in the magnitudes of UHI in the western and eastern suburbs were caused by the cooler rural air transport (first from NW then from E-NE) according to the changed wind direction. The phenomenon of the two peaks was observed in the course of the fall measurement and it could be explained only by the temporary weakening of the wind.

Connection between phenological phases and urban heat island in Debrecen and Szeged, Hungary (Lakatos, Gulyás 2003):

The study presumed that the urban climatic modification (UHI) affects the phenological and phenometrical properties of the urban vegetation. The phenological and temperature observations were taken in grid networks in the spring of 2003 in Szeged and Debrecen. As a good observable plant, *Forsythia suspensa* was the object of the examination because this plant occurred in 60-70% of the city areas. The timing of the different phenological phases was monitored in a daily fashion. According to the results there was close connection between the spatial distributions of the timing of these phenological phases and the UHI intensity. The strongest correlation occurred between the UHI intensity and the date of 100% flowering.

A multiple linear statistical model for estimating mean maximum urban heat island (Bottyán, Unger 2003); A statistical approach for estimating mean maximum urban temperature excess (Bottyán et al. 2003):

These studies examined the spatial and quantitative influence of urban factors on the air temperature field of Szeged using mobile measurements under different weather conditions in the periods of March 1999 – February 2000 and April–October 2002. Tasks included: (1) determination of spatial distribution of mean diurnal maximum UHI intensity and some urban surface parameters (built-up and water surface ratios, sky view factor, building height) using the standard Kriging procedure, as well as (2) development of statistical models in the heating and non-heating seasons using the above mentioned parameters and their areal extensions. Model equations were determined by means of stepwise multiple linear regression analysis. In both seasons the patterns of the mean UHI intensity had concentric shapes with some local irregularities. The intensity reached more than 2.1°C (heating season) and 3.1°C (non-heating season) in the centre of the city. As the measured and calculated UHI intensity patterns showed, there was clear connection between the spatial distribution of the the urban thermal excess and the examined land-use parameters, so these parameters played an important role in the evolution of the strong UHI intensity field. From the above mentioned parameters the sky-view factor and the building height were the most determining factors which were in line with the urban surface energy balance. Therefore, by means of these models there would be possibilities to predict mean maximum UHI intensity in other cities, which have land-use features similar to Szeged.

Intra-urban relationship between surface geometry and urban heat island: review and new approach (Unger 2004):

This paper provided a comprehensive review of the intra-urban sky view factor (SVF)–temperature relationship. Then a new approach to reveal the real connection between SVF and air temperature in an entire city was presented. The results found in the literature

were rather contradictory, possibly due the fact that previous investigations were limited to the central or specific parts (e.g. inner city, urban canyons) of cities and used few sites and measurements. Comparisons were often based on element pairs measured at selected sites. In some cases areal means were also discussed, but always in connection with one of the variables examined. For comparison, this study in Szeged utilized large number of areal means of SVF and air temperature. The values were related to almost a whole city and based on numerous measurements. The results showed a strong relationship in the intra-urban variations of these variables, i.e. urban surface geometry was a significant determining factor of the air temperature distribution inside a city if the selected scale was appropriate. Therefore, investigations of a sufficient number of appropriate-sized areas covering the largest part of a city or the entire city are needed to draw well-established conclusions.

Modelling of the annual mean maximum urban heat island with the application of 2 and 3D surface parameters (Unger 2006); Modelling the maximum development of urban heat island with the application of GIS based surface parameters in Szeged (Part 1): Temperature, surveying and geoinformational measurement methods (Balázs et al. 2005); Modelling the maximum development of urban heat island with the application of GIS based surface parameters in Szeged (Part 2): Stratified sampling and the statistical model (Gál et al. 2005):

The primary aim of these studies was to reveal quantitatively what effect urban structure had on the development, magnitude and spatial distribution of the annual mean maximum UHI using a selected representative sample area in Szeged. In order to quantify the effect mentioned above, besides the earlier applied SVF and different built-up parameters, a relatively new surface parameter (weighted volumetric compactness) was used to characterise the volume, structure and thermodynamical role of buildings. The calculation of this new parameter required a large-sized digital database that includes building's 3D measurement. Because this would take a long time, the research concentrated on a smaller but representative sample area, as the first step: the compactness of approximately 11,000 buildings in one third of the city was determined by geoinformational analysis. A stepwise multiple linear regression model was used to determine to what extent each parameter added to the annual mean UHI intensity. According to the results, there were clear connections between the spatial distribution of the UHI and the examined parameters (built-up and water surface ratios and weighted volumetric compactness), so these parameters played important role in the evolution of the UHI intensity field. The connection between compactness and the annual mean ('all weather') UHI intensity is stronger than with the SVF. Using the final model equation, the absolute deviations of the generated UHI (calculated for an independent one year period) remained under 0.5°C throughout almost the entire investigated area. The estimated UHI pattern with its characteristic features showed clear similarities to the real conditions.

Connection between urban heat island and sky view factor approximated by a software tool on a 3D urban database (Unger 2009); Relationship between the urban surface and the heat island in Szeged, Part 1: GIS procedure for quantifying surface geometry (Unger et al. 2006b); Relationship between the urban surface and the heat island in Szeged, Part 2: connection between surface geometry and temperature distribution (Unger et al. 2006a):

These studies provided a review on methods of SVF determination and intra-urban surface geometry–air temperature relationship. Then, a software-based method of SVF estimation from a 3D database, describing urban surface elements, was applied. Finally, related investigations in Szeged and importance of the results obtained were discussed. Previous investigations were limited to only specific urban parts or some canyons and used small numbers of sites and few occasions of measurements. This study utilized large number of areal means of SVF and temperature related to a large sample area and based on numerous measurements. The investigation revealed a strong relationship between these variables. Thus, surface geometry was a significant determining factor of the temperature distribution if the selected scale was appropriate.

Simulation of the mean urban heat island using 2D surface parameters: empirical modeling, verification and extension (Balázs et al. 2009):

In this paper the spatial distribution of the annual mean UHI intensity was simulated applying empirical models based on datasets from urban areas of Szeged and Debrecen, using simple and easily determinable urban surface cover variables. These two cities have similar topographic and climatic conditions. Temperature field measurements were carried out, Landsat satellite images were evaluated, and then one- and multi-variable models were constructed using linear regression techniques. The selected multiple-parameter models were verified using independent datasets from three urban settlements near Debrecen. In order to obtain some impression of the mean UHI patterns in other cities with no temperature measurements available, the best model among the obtained ones was extended to four urban areas situated in geographical environments similar to Szeged and Debrecen. The main shortcoming of typical empirical models, namely that they were often restricted to a specific location, was overcome by the obtained model since it was not entirely site but more region specific, and valid in a large region (Great Hungarian Plain) with several cities.

Computing continuous sky view factor using 3D urban raster and vector data bases: comparison and application to urban climate (Gál et al. 2009):

The use of high resolution 3D urban raster and vector databases in urban climatology was presented. The study applied two different methods to the calculation of continuous SVFs, compared their values and considered their usefulness and limitations in urban climate studies. It evaluated the relationship between urban geometry, quantified by SVF, and intra-urban nocturnal temperature variations using areal means in the whole urban area of Szeged. Results from the vector and raster models showed similar SVF values. The usefulness of application of areal means in SVF–temperature relations was confirmed. The vector and the raster approaches to the derivation of areal means of SVF were both showed to be powerful tools to obtain a general picture of the geometrical conditions in urban environments.

Analysis of the relationship between urban land use and urban heat island using GIS methods in Szeged (Mucsi et al. 2009):

In this paper, instead of traditional per-pixel classifiers, Normalized Endmember Spectral Mixture Analysis was applied to map urban land cover using Landsat TM data acquired over the city of Szeged. Impervious surface, one of the most important elements of VIS model, has been recognized as a key indicator in assessing urban environment. Fractional

images of impervious surfaces developed from LTM images (acquired in 1986 and 2007) were compared. The urban land cover map was the base of the spatial analysis of UHI, which demonstrated a very strong connection between the spatial distribution of main urban land cover classes and the spatial characteristics of UHI. In addition to 2D spatial analysis, the investigation was extended to include 3D urban surface analysis to assess the effect of urban surface geometry onto the UHI using geoinformatic methods. According to the results, there was a strong relationship in the intra-urban variations of surface geometry and heat island intensity.

Modeling of the urban heat island pattern based on the relationship between surface and air temperatures (Unger et al. 2010); City of sunlight after sunset – mapping of urban heat island using aerial remote sensing method in Szeged (Rakonczai et al. 2009):

The aim of these studies was to develop a new method for early nighttime near-surface air temperature pattern estimation based on surface temperature data in urban areas. The surface temperature data were collected by an airplane-based thermal infrared sensor at an altitude of 2000 m above ground level. The study area was covered by hundreds of images with a spatial resolution of about 2 m. The measured values were calibrated with data of in situ surface measurements of different land use types. Large temperature differences were found between green areas and densely built-up parts of the city. The structure of the city was reflected in the temperature map; roads and squares showed very high temperatures, while parks and waterbodies were up to 20 degrees cooler. Simultaneous air temperature measurements were carried out using a car-based temperature sensor along an almost 12 km long N-S urban transect. The measured points were located using a GPS device. Data were processed with GIS methods, including newly developed algorithms. In order to find the relationship between air and surface temperature a wider environment, the source area which determines the air temperature at a given point and time was taken into account. Using a source area with a radius of 500 m, a strong relationship was detected between the two parameters. Namely, the temperatures of the surfaces found in the surroundings (weighted by the distance) determine the temperature of the air parcel located at a given point. The obtained regression equation was applied to extend the results in order to model the air temperature field in a larger urban area of Szeged.

Comparison and generalisation of spatial patterns of the urban heat island based on normalized values (Unger et al. 2010); Investigation of the structure of an urban heat island using normalized intensity (Sümeghy, Unger 2004); Classification of the urban heat island patterns (Sümeghy, Unger 2003c):

The studied medium-sized cities (Szeged and Debrecen, Hungary) are located on a low and flat plain. Data were collected by mobile measurements in grid networks under different weather conditions between April 2002 and March 2003 in the time of daily maximum development of the UHI. Tasks included: (i) interpretation and comparison of the average UHI intensity fields using absolute and normalized values; (ii) classification of individual temperature patterns into generalized types by cities using normalization and cross-correlation. According to the results, spatial distribution of the annual and seasonal mean UHI intensity fields in the studied period had concentric shape with some local irregularities. The UHI pattern classification reveals that several (eight) types of the structure

could be distinguished in both cities. Shifts in the shape of patterns in comparison with the centralized pattern were in connection with the prevailing wind directions.

Evaluation of the thermal features of the local climate zones – a Szeged case study (Lelovics et al. 2013):

In this study the connection between air temperature of the urban area and its built-up features was examined in Szeged. Air temperature was measured along a N-S transect during anticyclonic situations in a mobil measurement campaign in 2008. The urban built-up features were characterized with the usage of LCZ system. The largest temperature values occurred in two areas: area at the edge of the LCZ 2 with densely located 3-4-storey buildings, and the parking lot of a shopping center at the border of LCZ 5 and LCZ 6 appeared as exceptionally warm spots.

Refining the concept of urban heat island using Local Climate Zone classification – examples from Szeged (Unger et al. 2014):

This study first presented the new LCZ classification system which reflected the climatic characteristics of the surfaces as well as its types and aspects of their separation based on quantified parameters. Secondly, it developed GIS methods which calculate these parameters for given areas. The database for these methods contained topographic map, 3D building and 2D road databases, as well as remotely sensed information from RapidEye satellite image. Thirdly, it determined the LCZ types occurring in the urbanized area of Szeged and were represented by circle areas with a diameter of 250 m. As a final step, it compared their thermal reactions based on the earlier temperature measurement campaigns. As a result, six built and one land cover LCZ types were distinguished in the studied urban area. Clear temperature differences occurred between these types. These differences were very significant on a day with favorable (calm and clear) weather conditions and they were more moderate using annual averages. These comparisons confirmed the usefulness of these type of classification: the thermal influence of any change or difference in landscapes were better expressed using LCZ difference concept than a simple but generally not clear urban-rural approach, and additionally, it provided an opportunity for intra- and inter-urban comparisons.

2.3. Studies based on the data of the second urban station network

Development, data processing and preliminary results of an urban human comfort monitoring and information system (Unger et al. 2015):

In this study the development and operation of an urban climate monitoring network and information system in Szeged and the related preliminary research results were discussed. The selection of the representative sites of the network was based primarily on the pattern of the LCZs in and around the city. After the processing of the incoming data (air temperature and relative humidity, as well as global radiation and wind speed), a human comfort index was calculated from the four meteorological parameters with a neural network method, then the measured and calculated parameters interpolated linearly into a regular grid with 500 m resolution. As public information, maps and graphs about the thermal and human comfort conditions appeared in 10-minute time steps as a real-time visualisation on the internet. As the preliminary case studies showed, the largest intra-urban thermal differences

occurred in the nocturnal hours reaching even 5°C in early spring. In the spatial distribution of human comfort conditions, there were distinct differences in the strength of the loading or favorable environmental conditions between the neighborhoods during the daytime. Finally, the utilization possibilities of the results were detailed.

Intra-urban temperature observations in two Central European cities: a summer study (Lelovics et al. 2016):

This paper presented an urban climatological application of the urban monitoring systems – recently implemented in Szeged and Novi Sad, Serbia – using the first set of data collected during the summer of 2014. In order to ensure a representative number and placement of stations, the selection of measurement sites was based on LCZ maps developed for both cities. This study concentrated only on the intra-urban temperature pattern characteristics expressed by the thermal reactions of the different LCZs in both cities. The daily temperature indices (e.g., summer days) had the highest values in the densely built-up LCZs. The diurnal cycle of surplus temperatures by LCZ classes under anticyclonic weather conditions was found to be similar in the two cities with higher absolute values in the case of Novi Sad. During summer, the diurnal variation of conventional UHI intensity confirmed the general knowledge that it remained positive with highest values at night, while negative values occurred predominantly during the day.

Urban heat island patterns and their dynamics based on an urban climate measurement network (Gál et al. 2016):

In this paper the spatial pattern of UHI and its dynamical background were analysed. Furthermore, the annual, seasonal and diurnal characteristics of UHI were examined according to the LCZs. The analysis was performed using one year (between June 2014 and May 2015) dataset from the measurement network of Szeged. This network consisted of 24 stations measuring air temperature and relative humidity. In the installation of the network the representativeness played an important role in order to that the stations represents their LCZs. The thermal reactions were examined during average and ideal conditions using the so-called weather factor. The results showed that the UHI was stronger in the compactly built zones and there were great differences between the zones. The greatest values appeared in summer, while the difference was small in winter. The UHI started to develop at sunset and existed through approximately 9–10 hours and differences were about 2°C larger in case of ideal days, when the conditions (wind, cloud cover) were appropriate to the strong development of the UHI. The cooling rates showed that the first few hours after sunset were determinative for the developing of UHI. In addition, the effect of UHI on annual mean temperature was also significant.

Employing an urban meteorological network to monitor air temperature conditions in the 'local climate zones' of Szeged, Hungary (Skarbit et al. 2017); Urban climate measurement network and information system in Szeged (Unger et al. 2017):

The average annual and seasonal air temperature conditions in the LCZs of Szeged were analysed. The basis of the analysis was a 1-year dataset from 2014 to 2015 from 20 station of the urban meteorological network. The network and its corresponding LCZ classes put temperature studies in Szeged into a new spatial framework to assess local climate and

UHI conditions. The stations were installed at locally representative sites using a Geographic Information System method based on the standard surface parameters of the LCZ classification. The network was purposely designed to monitor thermal differences among LCZ classes. Detailed site metadata were provided for each of the stations used in the analysis. The results showed that the densely built-up LCZs had higher annual and monthly mean and minimum air temperatures than structurally open and more vegetated classes, with nocturnal differences of $>4^{\circ}\text{C}$ observed under calm, clear skies. Among select temperature indices measured in the urban LCZ classes, frost days, cooling degree-days, and tropical nights differed markedly from the background rural LCZs. This difference suggested that local climatologies existed within the city, and that these had implications for thermal comfort, urban energy use, and urban agriculture. In addition, the dynamics of the UHI pattern was also presented at a night with ideal weather conditions. Finally, the evaluation of heating and cooling rates in Szeged showed an important role for LCZs in UHI analysis.

Comparison of regional and urban outdoor thermal stress conditions in heatwave and normal summer periods: A case study (Unger et al. 2020):

This study compared the diurnal variation of thermal stress conditions during a heatwave period (HW) to the ones during a normal summer period in the region and within the urban area of Szeged based on urban monitoring network data. Thermal stress categories of human bioclimatological index PET were adapted to the local population. Variation of the nocturnal intra-urban PET-patterns was analyzed along with the evolving UHI. A definite regional difference was found in the thermal stress conditions between the two periods, which was at least one PET-category in the daytime, while slightly less during the night. The nocturnal stress was higher in the inner city parts for both periods and the evolving UHI patterns determined the PET-patterns in a great extent. The UHI proved to be much stronger in the HW period. In summary, during the HW the nocturnal thermal stress on the urban inhabitants, especially those living in ‘hot spot’ neighborhoods, was significantly higher than what could be deducted from temperature data measured near the city. These types of results could provide valuable information for urban planners and decision-makers for evolving strategies against the adverse effects of urban climate and climate change to create livable settlements.

2.4. Studies based on local-scale simulation data

Projection of intra-urban modification of nighttime climate indices during the 21st century (Skarbit, Gál 2016):

This paper evaluated the alteration of certain nighttime climate indices namely warm nights ($T_{\min} \geq 17^{\circ}\text{C}$) and tropical nights ($T_{\min} \geq 20^{\circ}\text{C}$) during the 21st century in Szeged. In this study the MUKLIMO_3 model was used, which ensured the modelling of the local scale processes in the examined area. In the model for the land use the LCZ system was applied. In order to analyze longer periods the cuboid method was applied, which is a dynamical-statistical downscaling technique. The calculated indices for 1981–2010 were based on measurements and for 2021–2050 and 2071–2100 from the EURO-CORDEX datasets. The study presented the results of Representative Concentration Pathways scenarios namely RCP4.5 and RCP8.5 and they showed that the highest values appeared in the city centre and the number of the days clearly increased in the 21st century especially according to scenario

RCP 8.5. The values depended on the built-up types and there were more days towards to the densely built-up LCZs. Moreover, considering the relative changes of the zones, larger changes appeared in sparsely built-up zones and natural surfaces.

Urban climate in Central European cities and global climate change (Bokwa et al. 2018):

This paper was the final report of the „Urban climate in Central European cities and global climate change” project with the aim to raise the public awareness on those issues in five Central European cities: Szeged, Brno (Czech Republic), Bratislava (Slovakia), Kraków (Poland) and Vienna (Austria). Within the project, complex data concerning local geomorphological features, land use and long-term climatological data were used to perform the climate modelling analyses using the model MUKLIMO_3. According to the predictions presented, an increase in heat load, expressed in mean annual number of summer days, was expected in urban areas of Central Europe. Mean values for particular study areas were expected to increase by 2100, comparing to 1971–2000, by 20–50 days, depending on the scenario used. The regional pattern of the predicted values of mean annual number of summer days showed dependence on latitude, i.e. for cities located in the northern part of the study area, the values were lower than for cities located in the south. The difference for mean values, for particular study areas, reached about 40 days. The local patterns showed the impact of both land use/land cover and relief. The largest values of mean annual number of summer days were observed in areas with intense built-up which were located in the valley floors. In rural areas, larger values occurred in the valleys than in the hill tops. The differences between the places with the lowest value and the largest value in particular cities reached 60–100 days, depending on the scenario used.

Heat load assessment in Central European cities using an urban climate model and observational monitoring data (Bokwa et al. 2019):

Diurnal variability of spatial pattern of air temperature was studied in five cities in Central Europe: Bratislava (Slovakia), Brno (Czech Republic), Kraków (Poland), Szeged and Vienna (Austria), during one of the heatwaves in 2015 (4–14 August), with the application of MUKLIMO_3 model. 8th August was chosen to study in detail the urban heat load at 10.00, 16.00, 22.00 and 4.00 CEST. LCZ concept was used to supply data for the model and for the interpretation of the results obtained. Model outcomes were validated with measurement data from 86 points belonging to the networks which operated in the cities studied. The results obtained showed that among urban LCZ, the highest heat load was observed for LCZ 2 and LCZ 3 from 16.00 to 4.00, while at 10.00 there was no such clear pattern. Unlike forested areas, open green areas can contribute to the generation of high air temperature: $> 35^{\circ}\text{C}$ during daytime and $> 30^{\circ}\text{C}$ during nighttime. Important factors controlling the intra-zonal and inter-zonal variability of air temperature in particular LCZs were the local environmental conditions. During the daytime, diversified relief in the area of the city and its vicinities generated higher heat load in the valleys’ floors than in areas located above, both in rural and urban areas. The same landforms experience lowered heat load during the nighttime due to air temperature inversions effect.

Projection of present and future daily and evening urban heat load patterns (Unger et al. 2020):

In this modeling study the recent and future daily and evening thermal climate of a Central-European city (Szeged) was investigated in terms of heat load modification by applying MUKLIMO_3 model to project daily and evening climate indices. For surface parameterization the LCZ scheme was used. The investigation encompassed three climatological time periods (1981–2010, 2021–2050 and 2071–2100) and two emission scenarios for future climate (RCP4.5 and RCP8.5). The results showed that highest index values appeared in the city centre and stretch to the NW direction (LCZs 2, 3 and 8) and they decreased towards the vegetated rural surfaces (mainly LCZ D). That is, the values depended on the zone types and there were more days towards the densely built-up LCZs. Also, a general temporal change could be detected as the index patterns showed the substantial increasing tendency for both indices towards the end of this century. This temporal change suggested a two-way conclusion: first, the increasing number of hot days means a strongly deteriorating change of unfavourable thermal conditions, and second, the change in the number of the evening index provides more opportunities for regeneration and leisure-time activities outdoors in the already thermally less stressful evening hours for the urban inhabitants. This study gave very illustrative examples on the expected climate changes during this century and these examples show that there were several sides to these changes in urban environments. Furthermore, they clearly proved that global or regional scale climate predictions without urban climate interactions do not have enough detailed information.

Analysis of urban heat island with meteorological forecast model in Szeged (Molnár et al. 2017):

Aim of the research was the application of Weather Research and Forecasting (WRF) model in urban scale in order to predict the UHI effect. Therefore, high-resolution, nested simulations were carried out in case of a Szeged in 2015. In this area, a detailed measurement dataset was available for the model validation process. In numerical weather predictions models the applied urban land use information was crucial. Consequently, it was essential to improve the details of canopy parameterization if the static data did not manage to represent precisely the urban forms in a specific area. High-resolution remote sensing products of Landsat 8 OLI/TIRS satellite and multiple GIS techniques were applied to determine the sufficient canopy values. Several simulations were made with different model setups and input geographical databases to fine-tune the model performance for optimal agreement with measured UHI parameters. The results suggested that the model reproduced reasonably well the UHI effect related to measurements in case of uninterrupted (anticyclonic) weather conditions.

Evaluation of a WRF-LCZ system in simulating urban effects under non-ideal synoptic patterns (Molnár et al. 2018):

The modelling of meteorological variables under non-ideal (e.g. characterized by cyclonal activity) synoptic patterns is always challenging. It is particularly true, when the simulations are performed on local or neighborhood scale. In this study the spatio-temporal distribution of UHI of Szeged was predicted by the WRF model during two period with different meteorological background. During the first, a thick and permanent fog layer was located over the Carpathian Basin. The second one was dominated by a Mediterranean low that has caused high sums of precipitation. The comparison of modelled and observed variables suggested that the computed outputs showed robust consistency with the

observations during the rainfall event. On the foggy days, however, WRF had difficulties to capture the daily variability of UHI intensity. It was due to the large underestimations of moisture circumstances.

Modeling of urban heat island using adjusted static database (Molnár et al. 2019a):

In this study the WRF model was applied to examine the spatial and temporal formation of UHI phenomenon in Szeged. In order to achieve a more accurate representation of complex urban surface properties in WRF, a modified static database (consists of land use and urban canopy parameters) had been developed using satellite images and building information. In the new database, the number of urban grids increased by 76% related to the default case. The urban landscape in WRF became more complex after employing two urban land use classes instead of only one. The modification of the default parameters of a single layer urban scheme revealed that urban fractions decreased in all urban categories, while street widths increased resulting in narrower urban canyons. For testing the impact of the modifications on near-surface temperature estimation, a four-day heatwave period was selected from 2015. The model outputs had been evaluated against the observations of the local urban climate monitoring system (UCMS). WRF with the modified parameters simulated most of the features of UHI reasonably well. In most cases, biases with the simulations of the adjusted static database tended to be significantly lower than with the default parameters. Additionally, during a longer time period (i.e., the summer of 2015) the extreme values of near-surface air temperature and maxima of UHI intensities were evaluated on the basis of an urban and a rural site of UCMS. It was concluded that the maxima and minima of observed near surface air temperature were underestimated (overestimated) by about 1–3°C at the urban (rural) site. The maxima of UHI intensities indicated cold biases on 86 of 91 days.

Integration of an LCZ-based classification into WRF to assess the intra-urban temperature pattern under a heatwave period in Szeged, Hungary (Molnár et al. 2019b):

In this study the LCZ system was incorporated into the WRF model in order to facilitate proper land surface information for the model integrations. After the calculation of necessary input canopy parameters, based on local static datasets, simulations were performed to test the model's performance in predicting near-surface air temperature (T_a) and UHI intensity (ΔT) under a heatwave period in July 2017. The modelled values were evaluated against the observations of the local urban climate monitoring system. The results suggested that WRF with a single-layer canopy scheme and the LCZ-based static database was able to capture the spatiotemporal variation of the aforementioned variables reasonably well. The daytime T_a was generally overestimated in each zone. At nights, slight overestimations (underestimations) occurred in LCZ 6, LCZ 9, and LCZ D (LCZ 2 and LCZ 5). The mean ΔT was underestimated in the nighttime; however, the daytime ΔT was estimated accurately. The mean maxima (minima) of ΔT were underestimated (overestimated) with around 1.5–2°C, particularly in LCZ 2 and LCZ 5. Some components of the surface energy budget were also computed to shed light on the inter-LCZ differences of T_a . It was concluded that the nocturnal ground heat flux was about five times higher in urban LCZs than in the rural LCZ D, which resulted in a reduced cooling potential over the urbanized areas.

How does anthropogenic heating affect the thermal environment in a medium-sized Central European city? A case study in Szeged, Hungary (Molnár et al. 2020):

Since the estimation of anthropogenic heating was always problematic in medium-sized cities because of data lacking, the study intended to test how much the omission of such data influences the physical consistency in a numerical model (WRF). It was hypothesized that anthropogenic heating was an important input for the model, even in a relatively small urban area, therefore three different approaches were adapted to quantify its spatiotemporal distribution over Szeged. Four numerical experiments were performed in the WRF coupled with the single layer canopy scheme, which included the calculated fluxes and an anthropogenic flux-free reference case. By comparing the experiments, there were the opportunity to determine the effects of different anthropogenic heating scenarios on certain meteorological variables near the surface and in the overlying urban boundary layer. The maximum anthropogenic heat release was estimated to be ranging between 0.6 and 31.2 Wm⁻², with higher values on winter days. This heat surplus contributed to a maximum increase of 1.5°C in the simulated near-surface air temperature. Depending on the rate of anthropogenic heat release, the urban boundary layer became deeper, and the mixing of heat and momentum was more efficient. The results demonstrated that without the consideration of anthropogenic heating, numerical simulations performed to cities similar to Szeged cannot be physically complete.

2.5. Studies based in part on other data sources

Airborne surface temperature differences of the different Local Climate Zones in the urban area of a medium sized city (Skarbit et al. 2015):

This paper presented a case study about the surface temperature characteristics of the different LCZs in Szeged. For the evaluation high resolution surface temperature data acquired by a low-cost small-format digital imaging system, measured in early night hours were applied. The map of LCZs for the study area was derived by an automatic GIS method for LCZ classification. The results showed that the different LCZ classes had different surface temperature characteristics. Among the densely populated LCZ classes the open low-rise had the lowest surface temperature, thus it could be the most favorable urban built-up type if the aim is the decrease the effect of the urban heat load.

Using local climate zones to compare remotely sensed surface temperatures in temperate and hot desert cities (Fricke et al. 2020a); Exploring thermal differences in cities with different climates based on LCZ classification concept and satellite data (Fricke et al. 2020b):

Surface classification using the LCZ system provided an appropriate approach for distinguishing urban and rural areas, as well as comparing the surface urban heat island (SUHI) of climatically different regions. The goal of the study was to compare the SUHI effects of two Central European cities (Szeged and Novi Sad, Serbia) with temperate climate (Köppen-Geiger's Cfa), and a city (Beer Sheva, Israel) with hot desert climate (BWh). LCZ classification was completed using World Urban Database and Access Portal Tools methodology and the thermal differences were analysed on the basis of the land surface temperature data of the Moderate Resolution Imaging Spectroradiometer sensor, derived on

clear days over a four-year period. This intra-climate region comparison showed the difference between the SUHI effects of Szeged and Novi Sad in spring and autumn. As the pattern of Normalised Difference Vegetation Index (NDVI) indicated, the vegetation coverage of the surrounding rural areas was an important modifying factor of the diurnal SUHI effect, and could change the sign of the urban-rural thermal difference. According to the inter-climate comparison, the urban-rural thermal contrast was the strongest during daytime in summer with an opposite sign in each season.

Model development for the estimation of urban air temperature based on surface temperature and NDVI – a case study in Szeged (Guo et al. 2020):

Predictive models for urban air temperature (T_{air}) were developed by using urban land surface temperature (LST) retrieved from Landsat-8 and MODIS data, NDVI retrieved from Landsat-8 data and T_{air} measured by 24 stations in Szeged. The investigation focused on summer period (June–September) during 2016–2019. The relationship between T_{air} and LST was analyzed by calculating Pearson correlation coefficient, root-mean-square error and mean-absolute error using the data of 2017–2019, then unary (LST) and binary (LST and NDVI) linear regression models were developed for estimating T_{air} . The data in 2016 were used to validate the accuracy of the models. Correlation analysis indicated that there were strong correlations at night and relatively weaker ones during the daytime. The errors between T_{air} and $LST_{\text{MODIS-Night}}$ was the smallest, followed by $LST_{\text{MODIS-Day}}$ and $LST_{\text{Landsat-8}}$, respectively. The validation results showed that all models could perform well, especially during nighttime with an error of less than 1.5°C. However, the addition of NDVI into the linear regression models did not significantly improve the accuracy of the models, and even had a negative effect. Finally, the influencing factors as well as temporal and spatial variability of the correlation between T_{air} and LST were analyzed. $LST_{\text{Landsat-8}}$ had a larger original error with T_{air} , but the regression model based on Landsat-8 had a stronger ability to reduce errors.

REFERENCES

- Balázs B, Gál T, Zboray Z, Sümeghy Z (2005) Modelling the maximum development of urban heat island with the application of GIS based surface parameters in Szeged (Part 1): Temperature, surveying and geoinformatical measurement methods. *Acta Climatol* 38-39:5-16
- Balázs B, Unger J, Gál T, Sümeghy Z, Geiger J, Szegedi S (2009) Simulation of the mean urban heat island using 2D surface parameters: empirical modeling, verification and extension. *Meteorol Appl* 16:275-287
- Bokwa A, Dobrovolny P, Gal T, Geletic J, Gulyas A, Hajto MJ, Holec J, Hollosi B, Kielar R, Lehnert M, Skarbit N, Stastny P, Svec M, Unger J, Walawender JP, Zuvella-Aloise M (2018) Urban climate in Central European cities and global climate change. *Acta Climatol* 51-52:7-35
- Bokwa A, Geletic J, Lehnert M, Zuvella-Aloise M, Hollósi B, Gál T, Skarbit N, Dobrovolný P, Hajto MJ, Kielar R, Walawender JP, Šťastný P, Holec J, Ostapowicz K, Burianová J, Garaj M (2019) Heat load assessment in Central European cities using an urban climate model and observational monitoring data. *Energy Build* 201:53-69
- Bottyán Z, Unger J (2003) A multiple linear statistical model for estimating mean maximum urban heat island. *Theor Appl Climatol* 75: 233-243
- Bottyán Z, Balázs B, Gál T, Zboray Z (2003) A statistical approach for estimating mean maximum urban temperature excess. *Acta Climatol* 36-37:17-26
- Fricke C, Pongrácz R, T Gál, S Savic, Unger J (2020a) Using local climate zones to compare remotely sensed surface temperatures in temperate and hot desert cities. *Morav Geogr Rep* 28:48-60

- Fricke C, Unger J, Pongrácz R (2020b) Eltérő éghajlatú városok termikus különbségeinek feltárása az LCZ osztályozás koncepciója és műholdas adatok alapján. [Exploring thermal differences in cities with different climates based on LCZ classification concept and satellite data. (in Hungarian)] *Légekör* 65:80-85
- Gál T, Balázs B, Geiger J (2005) Modelling the maximum development of urban heat island with the application of GIS based surface parameters in Szeged (Part 2): Stratified sampling and the statistical model. *Acta Climatol* 38-39:59-69
- Gál T, Lindberg F, Unger J (2009) Computing continuous sky view factor using 3D urban raster and vector data bases: comparison and application to urban climate. *Theor Appl Climatol* 95:111-123
- Gál T, Skarbit N, Unger J (2016) Urban heat island patterns and their dynamics based on an urban climate measurement network. *Hung Geogr Bull* 65/2:105-116
- Guo Y, Gál T, Tian G, Li F, Unger J (2020) Model development for the estimation of urban air temperature based on surface temperature and NDVI – a case study in Szeged. *Acta Climatol* 54:29-40
- Károssy Cs, Gyarmati Z (1980) Városi hősziget kialakulása Szeged légtérében. [Development of urban heat island in the air of Szeged. (in Hungarian)] *JGYTF Tudományos Közleményei*, 111-120
- Lakatos L, Gulyás Á (2003) Connection between phenological phases and urban heat island in Debrecen and Szeged, Hungary. *Acta Climatol* 36-37:79-83
- Lelovics E, Unger J, Gál T (2013) A lokális klímazónák termikus sajátosságainak elemzése – szegedi esettanulmány. [Evaluation of the thermal features of the local climate zones – a Szeged case study. (in Hungarian)] *Légekör* 58/4, 140-144
- Lelovics E, Unger J, Savic S, Gál T, Milosevic D, Gulyás Á, Markovic V, Arsenovic D, Gál CV (2016) Intra-urban temperature observations in two Central European cities: a summer study. *Időjárás* 120:283-300
- Molnár G, Gál T, Gyöngyösi AZ (2018) Evaluation of a WRF-LCZ system in simulating urban effects under non-ideal synoptic patterns. *Acta Climatol* 51-52:57-73
- Molnár G, Gyöngyösi AZ, Gál T (2017) A városi hősziget vizsgálata meteorológiai modell segítségével Szegeden [Analysis of urban heat island with meteorological forecast model in Szeged. (in Hungarian)] *Légekör* 61:130-135
- Molnár G, Gyöngyösi AZ, Gál T (2019a) Modeling of urban heat island using adjusted static database. *Időjárás* 123:371-390
- Molnár G, Gyöngyösi AZ, Gál T (2019b) Integration of an LCZ-based classification into WRF to assess the intra-urban temperature pattern under a heatwave period in Szeged, Hungary. *Theor Appl Climatol* 138:1139-1158
- Molnár G, Kovács A, Gál T (2020) How does anthropogenic heating affect the thermal environment in a medium-sized Central European city? A case study in Szeged, Hungary. *Urban Clim* 34:100673
- Mucsi L, Unger J, Henits L (2009) A beépítettség és a városi hősziget kapcsolatrendszerének vizsgálata geoinformatikai módszerekkel Szegeden. [Analysis of the relationship between urban land use and urban heat island using GIS methods in Szeged. (in Hungarian)] *Földrajzi Közlemények* 113:411-429
- Oke TR (1987) *Boundary Layer Climates*. Second Edition. Routledge, University Press, Cambridge
- Pelle L (1983) Városklíma mérések Szegeden. [Urban climate measurements in Szeged. (in Hungarian)] *Légekör* 28:10-12
- Rakonczi J, Unger J, Mucsi L, Szatmári J, Tobak Z, van Leeuwen B, Gál T, Fiala K (2009) A napfény városa naplemente után – légi távérzékeléses módszerrel támogatott hősziget-térképezés Szegeden. [City of sunlight after sunset – mapping of urban heat island using aerial remote sensing method in Szeged. (in Hungarian)] *Földrajzi Közlemények* 113:367-383
- Skarbit N, Gál T (2016) Projection of intra-urban modification of nighttime climate indices during the 21st century. *Hung Geogr Bull* 65:181-193
- Skarbit N, Gál T, Unger J (2015) Airborne surface temperature differences of the different Local Climate Zones in the urban area of a medium sized city. In: 2015 Joint Urban Remote Sensing Event. North Conway (NH), USA: IEEE Service Center, Paper: 7120497, 4 p
- Skarbit N, Stewart ID, Unger J, Gál T (2017) Employing an urban meteorological network to monitor air temperature conditions in the 'local climate zones' of Szeged, Hungary. *Int J Climatol* 37/S1:582-596
- Sümegehy, Unger (2003a) Seasonal case studies on the urban temperature cross-section. *Acta Climatol* 36-37:101-109
- Sümegehy Z, Unger J (2003b) A települések hőmérséklet-módosító hatása – a szegedi hősziget-kutatások tükrében. [Temperature modification effect of settlements – heat island investigations in Szeged. (in Hungarian)] *Földrajzi Közlemények* 127/51:23-44
- Sümegehy, Unger (2003c) Classification of the urban heat island patterns. *Acta Climatol* 36-37:93-100

*Urban heat island studies in Szeged, Hungary –
An overview based on papers published over the past forty years (1980–2020)*

- Sümeghy Z, Unger J (2004) A városi hősziget szerkezetének vizsgálata normalizált intenzitás segítségével. [Investigation of the structure of an urban heat island using normalized intensity. (in Hungarian)] *Légekör* 49/2:15-19
- Unger J (1992a) The seasonal system of urban temperature surplus in Szeged, Hungary. *Acta Climatol* 24-26:49-57
- Unger J (1992b) Diurnal and annual variation of the urban temperature surplus in Szeged, Hungary. *Időjárás* 96:235-244
- Unger J (1996a) Heat island intensity with different meteorological conditions in a medium-sized town: Szeged, Hungary. *Theor Appl Climatol* 54:147-151
- Unger J (1996b) A városi hősziget és a szél kapcsolata Szeged példáján. [Relationship between urban heat island and wind on the example of Szeged. (in Hungarian)] *Légekör* 41/4:21-23
- Unger J (1997) A városi hősziget hatása a fűtési energiaigényre Szegeden. [The effect of urban heat island on heating energy demand in Szeged. (in Hungarian)] *Légekör* 42/2:18-19
- Unger J (2004) Intra-urban relationship between surface geometry and urban heat island: review and new approach. *Clim Res* 27:253-264
- Unger J (2006) Modelling of the annual mean maximum urban heat island with the application of 2 and 3D surface parameters. *Clim Res* 30:215-226
- Unger J (2009) Connection between urban heat island and sky view factor approximated by a software tool on a 3D urban database. *Int J Environ Poll* 36:59-80
- Unger J, Makra L (2007) Urban-rural difference in the heating demand as a consequence of the heat island. *Acta Climatol* 40-41:155-162
- Unger J, Ondok J (1995) Some features of urban influence on temperature extremities. *Acta Climatol* 28-29:63-76
- Unger J, Sümeghy Z (2001) A városi hőmérsékleti többlet: keresztmetszet menti vizsgálatok Szegeden. [Urban temperature surplus: cross-sectional studies in Szeged. (in Hungarian)] *Légekör* 46/4:19-25
- Unger J, Bottyán Z, Gulyás Á, Kevei-Bárány I (2001a) Urban temperature excess as a function of urban parameters in Szeged, Part 2: Statistical model equations. *Acta Climatol* 34-35: 15-21
- Unger J, Bottyán Z, Sümeghy Z, Gulyás Á (2000) Urban heat island development affected by urban surface factors. *Időjárás* 104:253-268
- Unger J, Bottyán Z, Sümeghy Z, Gulyás Á (2004) Connection between urban heat island and surface parameters: measurements and modeling. *Időjárás* 108:173-194
- Unger J, Bottyán Z, Sümeghy Z, Gulyás Á, Fogarasi S, Sódar I (1999a) A model for the maximum urban heat island in Szeged, Hungary. *Proceed Berzsényi Dániel Teacher Training College Szombathely, Natural Science Brochures* 4:31-38
- Unger J, Gál T, Csépe Z, Lelovics E, Gulyás Á (2015) Development, data processing and preliminary results of an urban human comfort monitoring and information system. *Időjárás* 119:337-354
- Unger J, Gál T, Geiger J (2006a) A városi felszín és a hősziget kapcsolata Szegeden, 2. rész: a felszíngeometria és a hőmérséklet-eloszlás kapcsolata. [Relationship between the urban surface and the heat island in Szeged, Part 2: connection between surface geometry and temperature distribution. (in Hungarian)] *Légekör* 51/4:8-14
- Unger J, Gál T, Kovács P (2006b) A városi felszín és a hősziget kapcsolata Szegeden, 1. rész: térinformatikai eljárás a felszíngeometria számszerűsítésére. [Relationship between the urban surface and the heat island in Szeged, Part 1: GIS procedure for quantifying surface geometry. (in Hungarian)] *Légekör* 51/3:2-9
- Unger J, Gál T, Rakonczai J, Mucsi L, Szatmári J, Tobak Z, van Leeuwen B, Fiala K (2010a) Modeling of the urban heat island pattern based on the relationship between surface and air temperatures. *Időjárás* 114:287-302
- Unger J, Lelovics E, Gál T, Mucsi L (2014) A városi hősziget fogalom finomítása a Lokális Klímazónák koncepciójának felhasználásával – példák Szegedről [Refining the concept of urban heat island using Local Climate Zone classification – examples from Szeged. (in Hungarian)] *Földrajzi Közlemények* 138/1:50-63
- Unger J, Pál V, Sümeghy Z, Kádár E, Kovács L (1999b) A maximális kifejlődésű városi hősziget területi kiterjedése tavasszal Szegeden. [The spatial extent of the maximally developed urban heat island in spring in Szeged. (in Hungarian)] *Légekör* 44/3:34-37
- Unger J, Skarbit N, Gál T (2017) Szegedi városklíma mérőállomás-hálózat és információs rendszer. [Urban climate measurement network and information system in Szeged. (in Hungarian)] *Légekör* 61:114-118
- Unger J, Skarbit N, Gál T (2020) Projection of present and future daily and evening urban heat load patterns. *Acta Climatol* 54:19-27
- Unger J, Skarbit N, Kovács A, Gál T (2020) Comparison of regional and urban outdoor thermal stress conditions in heatwave and normal summer periods: A case study. *Urban Clim* 32:100619

- Unger J, Sümeghy Z, Gulyás Á, Bottyán Z, Mucsi L (2001b) Land-use and meteorological aspects of the urban heat island. *Meteorol Appl* 8:189-194
- Unger J, Sümeghy Z, Mucsi L, Pál V, Kádár E, Kevei-Bárány I (2001c) Urban temperature excess as a function of urban parameters in Szeged, Part 1: Seasonal patterns. *Acta Climatol* 34-35:5-14
- Unger J, Sümeghy Z, Szegedi S, Kiss A, Gécz R (2010b) Comparison and generalisation of spatial patterns of the urban heat island based on normalized values. *Physics and Chemistry of the Earth* 35:107-114
- Unger J, Sümeghy Z, Zoboki J (2001e) Temperature cross-section features in an urban area. *Atmos Res* 58:117-127